

Chimeric Leader Peptides for the Generation of Non-Natural Hybrid RiPP Products

Supporting information

Brandon J. Burkhart^{†‡}, Nidhi Kakkar[†], Graham A. Hudson[†], Wilfred A. van der Donk^{†‡},
Douglas A. Mitchell^{†‡}

[†]Department of Chemistry, University of Illinois at Urbana-Champaign, 600 South
Mathews Avenue, Urbana, Illinois 61801, USA.

[‡]Carl R. Woese Institute for Genomic Biology, University of Illinois at Urbana-
Champaign, 1206 West Gregory Drive, Urbana, Illinois 61801, USA.

Table of Contents

Methods.....	3
Table S1. New plasmids generated for this study.....	8
Table S2. Nucleotide sequences	9
Figure S1. Natural “hybrid” RiPP biosynthetic gene clusters	11
Figure S2. Structure and precursor peptide of nisin.	13
Figure S3. Structure and precursor peptide of subtilisin A.....	14
Figure S4. Hyp2.1 co-expression with HcaD/F and AlbA at high and low aeration.....	15
Figure S5. MS/MS of thiazoline-modified sactipeptide Hyp2.2.	16
Figure S6. GluC digestion of thiazoline-modified and thioether-crosslinked Hyp 2.2.	18
Figure S7. Structure and precursor peptide of two prochlorosins.	19
Figure S8. Optimization of HcaD/F-ProcM co-expression and plasmid design.	20
Figure S9. MS/MS fragmentation of thiazoline/lanthionine in modified Hyp3.1	21
Figure S10. MALDI-TOF-MS analysis of thiazoline/lanthionine modified Hyp3.2	22
Figure S11. MS/MS fragmentation of thiazoline/lanthionine in modified Hyp3.2.	23
Figure S12. Thiazoline and lanthionine product mixtures produced with Hyp4.1 and Hyp4.2.	25
Figure S13. MS/MS fragmentation of modified Hyp4.1a.	26
Figure S14. MS/MS fragmentation of modified Hyp4.3a.	28
Figure S15 MS/MS fragmentation of modified Hyp4.3a after thermolysin digestion.	30
Figure S16. GC-MS analysis of Hyp3.3 MeLan.....	32
Figure S17. MS/MS fragmentation of Hyp4.3 minor products	33
Figure S18. MS/MS fragmentation of thiazoline/lanthionine modified Hyp3.3	35
Figure S19. Design and production of decarboxylated linear azol(in)e-containing peptide.	36
References.....	37

Methods

General methods. Materials were purchased from Fisher Scientific, Gold Biotechnology, or Sigma-Aldrich unless otherwise noted. Tryptone and yeast extract were purchased from Dot Scientific. Restriction enzymes (REs), AspN endoprotease, Q5 polymerase, T4 DNA ligase, and deoxynucleotides (dNTPs) were purchased from New England Biolabs (NEB). Oligonucleotide primers were synthesized by Integrated DNA Technologies (IDT) and are listed in Table S2. DNA spin columns were purchased from Epoch Life Sciences, and DNA sequencing was performed by the Roy J. Carver Biotechnology Center (UIUC). All polymerase chain reactions (PCRs) were conducted on an S1000 thermal cycler (Bio-Rad).

Cloning. Plasmids were constructed using REs and DNA ligase or by Gibson assembly (GA). For RE cloning, the target gene was amplified with Q5 polymerase, and after PCR cleanup using the QIAquick PCR Purification Kit Protocol, the amplicon was digested with restriction enzymes for ligation into a similarly digested and purified vector. For amplifications which gave more than one product, a gel extraction was performed. Ligations were performed with T4 DNA ligase at 23 °C for 1 h (100 ng vector and 3-fold excess insert). For GA, the standard protocol was followed with guidance from the NEBuilder Assembly tool (nebuilder.neb.com). Inserts were generated using Q5 polymerase and purified as above. Vector backbones were linearized using PCR or restriction enzymes and similarly purified.

Genes for the cyclodehydratase (HcaF and HcaD),¹ lanthipeptide synthetase (ProcM and NisB/C),² dehydroalanine reductase (NpnJ),³ and flavoenzyme decarboxylase (MibD)⁴ were cloned previously from their native organisms. All new plasmids used in this study are listed in Table S1 and were constructed using primers listed in Table S2. The subtilisin radical SAM gene (AlbA) and its precursor peptide (SboA) were cloned from *Bacillus subtilis* strain 168 genomic DNA.

The hybrid peptides were built from HcaA, SboA, or ProcA precursor peptides through overlap extension PCR and initially cloned into a modified pET28 vector with an N-terminal maltose-binding protein (MBP) affinity tag (pET28-MBP). This intermediate was then used to clone MBP-tagged hybrid peptides into duet vectors or to express the peptide for in vitro activity assays. The NisA-derived hybrid peptide was synthesized as a gblock (IDT) for subsequent cloning and was cloned directly into a duet vector in frame with a His₆ tag. Duet vectors pACYCDuet, pCDFDuet, pETDuet, and pRSFDuet were used for co-expression in *E. coli* (see Table S1), as has been well established,⁵ and genes were sequentially cloned into each multiple cloning site. To insert the cyclodehydratase HcaF and HcaD genes into a single multiple cloning site, the genes were taken together as a single amplicon from pETDuet-HcaF-HcaD.

Site-directed mutagenesis. Changes to the sequence of hybrid peptides were made with cloned PFU or KOD polymerase (a proofreading DNA polymerase isolated from *Thermococcus kodakaraensis*) and the site-directed mutagenesis (SDM) primers in Table S2 following the Agilent QuikChange protocol.

In vivo production of modified hybrid peptides. BL21(RIPL-DE3) chemically competent cells were co-transformed with pairs of duet vectors (Table S2) and selected with 100 µg/mL ampicillin for pETDuet, 50 µg/mL kanamycin for pRSFDuet or pET28, and 34 µg/mL chloramphenicol for pACYCDuet. Initial cultures were started from single colonies and grown in 10 mL of Luria–Bertani (LB) broth in 18 mm glass culture tubes at 37 °C supplemented with appropriate antibiotics for several hours, and then used to inoculate 0.5 or 1 L of the same media. Cells were grown to ~0.8 OD₆₀₀, put on ice for 10 min, and induced with 0.6 mM IPTG (isopropyl β-D-1-thiogalactopyranoside) at 22 °C except for co-expressions containing AlbA, which were shaken at 100 rpm in non-baffled flasks to reduce aeration (see Figure S3).⁶ After 18 h induction, cells were harvested at 4000 × g for 15 min at 4 °C, washed with TBS (Tris-buffered saline: 25 mM Tris pH 8.0, 150 mM NaCl), and centrifuged again at 4000 × g for 10 min at 4 °C. Cell pellets were stored for up to 1 week at -20 °C.

Protein expression and purification. BL21(DE3-RIPL) cells were transformed with plasmids containing the tagged proteins and selected using appropriate antibiotics. Starter cultures were grown in 10 mL LB with antibiotics and used to inoculate 1 L of similarly prepared media. After reaching an OD₆₀₀ of ~0.8, cells were induced overnight with IPTG. Next, cells were harvested by centrifugation at 4000 × g for 15 min at 4 °C, washed with TBS, and then subjected to centrifugation at 4000 × g for 10 min at 4 °C. Cell pellets were stored for up to 1 week at -20 °C. Proteins used for in vitro assays were purified using affinity chromatography via the MBP or His₆ tag.

MBP-tagged proteins were purified from *E. coli* cells using amylose resin (NEB). The resin was pre-equilibrated with 5 bed volumes of Buffer A [50 mM Tris pH 7.5, 500 mM NaCl, 2.5% (v/v) glycerol, 0.1% (v/v) Triton X-100]. Cell pellets were suspended in Buffer A and sonicated 3 times for 30 seconds at 10-13 W using a Misonix MICROSON XL2000 Cell Disruptor with 10 min incubations at 4 °C between each 30 second sonication period to prevent sample heating. The lysate was clarified by centrifugation at 34000 × g for 1 h on a Sorvall RC 6 plus centrifuge, applied to the equilibrated resin, and washed with 10 bed volumes of Buffer B [50 mM Tris pH 7.5, 400 mM NaCl, 2.5% (v/v) glycerol]. Protein was then eluted using Elution Buffer [50 mM Tris pH 7.5, 300 mM NaCl, 2.5% (v/v) glycerol, 10 mM maltose] and collected into Amicon Ultra 15 mL Filter centrifugal filters [30kDa NMWL (Nominal Molecular Weight

Limit)]. The eluted protein was concentrated and a 10-fold buffer exchange was performed into Storage Buffer [50 mM HEPES, 300 mM NaCl, 2.5% (v/v) glycerol] through centrifugation at $4000 \times g$. The final protein concentration was calculated from the absorbance at 280 nm (NanoDrop 2000 UV-Vis Spectrophotometer) with the predicted protein extinction coefficient (<http://web.expasy.org/protparam/>) and the Bradford assay (Pierce™ Coomassie Protein Assay Kit). All proteins were stored at $-80\text{ }^{\circ}\text{C}$. Note that after initial column loading, all wash and storage buffers were supplemented with 1 mM tris-(2-carboxylethyl)-phosphine (TCEP).

His₆-tagged proteins were purified identically to the above protocol except the buffer composition differed as follows: Buffer A [50 mM Tris pH 7.5, 500 mM NaCl, 2.5% (v/v) glycerol, 15 mM imidazole], Buffer B [50 mM Tris pH 7.5, 400 mM NaCl, 2.5% (v/v) glycerol, 30 mM imidazole], and Elution Buffer [50 mM Tris pH 7.5, 300 mM NaCl, 2.5% (v/v) glycerol, 250 mM imidazole].

Purification of modified hybrid peptides. All hybrid peptides except Hyp1.1 were MBP-tagged and purified as described above. Typically, >20 mg of MBP-tagged peptide (corresponding to >1 mg of core peptide after affinity tag removal) was obtained from 1 L of culture. Hyp1.1 was expressed as a His₆-tagged peptide and purified by the following procedure. The harvested cells were resuspended in 25 mL of LanA Buffer 1 [6 M guanidine hydrochloride, 20 mM NaH₂PO₄, pH 7.5 at 25 °C, 500 mM NaCl, 0.5 mM imidazole], and lysed by sonication (50% amplitude, 1.0 s pulse, 2.0 s pause, 5 min). The sample was subjected to centrifugation ($23,700 \times g$ for 30 min at 4 °C) and the supernatant containing the His₆-tagged peptide was retained for further purification. The His₆-tagged peptide was then purified by immobilized metal affinity chromatography (IMAC) using 2-4 mL of His60 Ni Superflow Resin (Clontech). The supernatant was applied to the column and the column was washed with 2 column volumes of LanA Buffer 1 followed by 2 column volumes of LanA Buffer 2 [4 M guanidine hydrochloride, 20 mM NaH₂PO₄, pH 7.5 at 25 °C, 300 mM NaCl, 30 mM imidazole], and then eluted with 3 column volumes of LanA Elution Buffer [4 M guanidine hydrochloride, 20 mM Tris, pH 7.5 at 25 °C, 100 mM NaCl, 1 M imidazole]. The elution fractions containing the peptide were desalted by Vydac C4 SPE column and lyophilized and stored at $-80\text{ }^{\circ}\text{C}$.

In vitro modification assays. In vitro assays were performed with purified proteins and peptides as described previously.^{1,3,7,8} In general, peptides were supplied at 50 μM. Proteins were present at 5 to 20 μM and allowed to react for 16 h. Reactions were carried out in synthetase buffer [50 mM Tris pH 7.5, 125 mM NaCl, 20 mM MgCl₂, 1 mM TCEP]. However, assays with the dehydroalanine reductase (NpnJ_A) were performed in 50 mM HEPES pH 7.4 with 1.5 mM NADPH.

MALDI-TOF-MS. Matrix-assisted laser desorption/ionization time of flight mass spectrometry (MALDI-TOF-MS) was used to analyze posttranslational modifications based on their characteristic mass changes and reactivity towards mild acid or iodoacetamide treatment.⁹ Upon in vitro or in vivo modification, peptides were digested with a commercial protease (AspN, ArgC, proteomics grade trypsin, GluC, or thermolysin) following the manufacturer's protocol. Hydrochloric acid (200 mM) or iodoacetamide (20 mM at 8 pH) were individually added to an aliquot of the digestion and allowed to react for 1 h in the dark at 22 °C. Next, the samples were desalted with a ZipTip (Millipore) according to the manufacturer's instructions and eluted into 3.5 μ L of 70 % MeCN. Then, 0.5 μ L was applied to a MALDI target plate with 1 μ L of matrix and subsequently mixed until crystallized. For the Hyp2.1 and Hyp2.2 peptides, the ideal matrix solution was 20 mg/mL sinapinic acid (SA) with 10 mg/mL 2,5-dihydroxybenzoic acid (DHB) in 70 % MeCN. All other peptides were applied with a matrix solution of 20 mg/mL of α -cyano-4-hydroxycinnamic acid (CHCA) and 10 mg/mL DHB in 60% MeCN. The samples were analyzed using a Bruker Daltonics UltrafleXtreme MALDI-TOF mass spectrometer in reflector/positive mode using the default RP900_4500_Da.par method.

High performance liquid chromatography (HPLC) purification of modified hybrid peptides. A subset of peptides were desalted and purified (>75%) for MS/MS characterization. Hyp3.2 was purified for determination of the stereochemistry of its MeLan (see below). The separations were performed on an Agilent 1200 series HPLC fitted with a 10 \times 250 mm Betasil C18 column (Fisher Scientific). A gradient elution was used with Buffer A (10 mM ammonium bicarbonate) and Buffer B (10 mM ammonium bicarbonate in 90% MeCN) according to the following linear gradient combinations: at t=0 min, 6% B; t=3.0 min, 6% B; t=6.0 min, 15% B; t=21.0 min, 40% B; t=24.0 min, 100% B; t=33.0 min, 100% B; t=37.0 min, 6% B; t=47.0 min, 6% B. Hyp3.x peptides eluted around 11 min whereas Hyp4.x eluted around 16 min. Hyp2.2 was purified using a different linear gradient combination: at t=0 min, 6% B; t=3.0 min, 6% B; t=7.0 min, 23% B; t=23.0 min, 52% B; t=26.0 min, 100% B; t=32.0 min, 100% B; t=37.0 min, 6% B; t=45.0 min, 6% B. Hyp2.2 eluted at 20 min. After elution from the column, the MeCN portion of the solvent was removed in a vacufuge (Eppendorf), and the remaining liquid was lyophilized using a FreeZone 4.5 L benchtop freeze dry system (Labconco).

HRMS and MS/MS analysis. HPLC-purified peptides or peptides desalted using a ZipTip were diluted 1:1 using ESI mix (80% MeCN, 19% water, 1% formic acid). Samples were directly infused into a ThermoFisher Scientific Orbitrap Fusion ESI-MS using an Advion TriVersa Nanomate 100. The MS was calibrated and tuned with Pierce LTQ Velos ESI Positive Ion Calibration Solution (ThermoFisher). The

MS was operated using the following parameters: resolution, 100,000; isolation width (MS/MS), 2 m/z; normalized collision energy (MS/MS), 35; activation q value (MS/MS), 0.4; activation time (MS/MS), 30 ms. Fragmentation was performing using collision-induced dissociation (CID) at 35%. Data analysis was conducted using the Qualbrowser application of Xcalibur software (Thermo-Fisher Scientific).

Determination of methyllanthionine stereochemistry. The stereochemistry of the MeLan in Hyp4.3a was determined according to previously reported methods,¹⁰ with slight modification. Briefly, after HPLC, the peptide sample was dissolved in 3 mL of 6 M DCl in D₂O (used to distinguish non-enzymatic epimerization products upon GC-MS analysis) and placed in a sealed glass pressure tube. This mixture was heated to 110 °C for 24 h without stirring. After being allowed to cool, the solvent was removed *in vacuo*. In a separate round bottom flask, acetyl chloride (1.5 mL) was added dropwise to MeOH (5 mL) at 0 °C with stirring. This solution (4 mL) was then added to the hydrolysate, which was again heated to 110 °C for 1 h. After cooling, the solvent was removed, and the residue was taken up in 3 mL of CH₂Cl₂. The suspension was then cooled to 0 °C and pentafluoropropionic acid (1 mL) was added dropwise. Next, the sample was heated to 110 °C for 30 min and allowed to cool. The solvent was again removed before suspending the derivatized product in MeOH (200 µL) prior to GCMS analysis.

The derivatized samples were analyzed by GC-MS (Agilent HP 6890N) using an Agilent CP-Chirasil-L-Val column (25 m × 0.25 mm × 0.12 µm), with co-injection of previously prepared DL-MeLan and LL-MeLan standards for stereochemical verification.¹¹ Samples were applied to the column via split injection and run according to the following temperature method: 150 °C injection for 3 min, then raised to 200 °C by 3 °C /min and held (21.6 min total runtime). The MS was operated using selected ion monitoring at 379 Da for the detection of MeLan isomers.

Table S1. New plasmids generated for this study and their use in combinations. Hybrid peptides (Hyp) are listed in Figure 2, 3, 4, 5 and S19. HcaF-HcaD comprise a two-component, thiazoline-forming cyclodehydratase, NisB and NisC form a class I lanthipeptide synthetase, while ProcM is a class II lanthipeptide synthetase. Constructs for the tailoring enzymes MibD and NpnJ_A are reported elsewhere.^{3,8} The combinations of plasmids used for co-expression and the figure where the results are presented are also listed. Abbreviations: No., number; MCS, multiple cloning site; MBP, maltose-binding protein.

No.	Name	Plasmid backbone (copy number ¹²)	Gene(s) MCS1; MCS2	Co-expression of plasmids; Figure for result
1	pACYC-B-C	pACYCDuet (10-12)	NisB; NisC	1+2+3; Fig. 2
2	pRSF-F-D	pRSFDuet (>100)	HcaF; HcaD	1+2+3; Fig. 2
3	pCDF-1.1	pCDFDuet (20-40)	His ₆ -Hyp1.1; (empty)	1+2+3; Fig. 2
4	pACYC-AlbA	pACYCDuet (10-12)	(empty); AlbA	See below
5	pET-2.1-FD	pETDuet (~40)	MBP-Hyp2.1; HcaF-HcaD	5+4; Fig. S4
6	pET-2.2-FD	pETDuet (~40)	MBP-Hyp2.2; HcaF-HcaD	6+4; Fig. 3
7	pET-3.1-FD	pETDuet (~40)	MBP-Hyp3.1; HcaF-HcaD	7+16; Fig. S4
8	pET-3.2-FD	pETDuet (~40)	MBP-Hyp3.2; HcaF-HcaD	8+16; Fig. S10
9	pET-3.3-FD	pETDuet (~40)	MBP-Hyp3.3; HcaF-HcaD	9+16; Fig. 4
10	pET-3.4-FD	pETDuet (~40)	MBP-Hyp3.4; HcaF-HcaD	10+11; Fig. S19
11	pCDF-MibD	pCDFDuet (20-40)	MibD; (empty)	10+11; Fig. S19
12	pET-4.1-FD	pETDuet (~40)	MBP-Hyp4.1; HcaF-HcaD	12+16; Fig. S12
13	pET-4.2-FD	pETDuet (~40)	MBP-Hyp4.2; HcaF-HcaD	13+16; Fig. S12
14	pET-4.3-FD	pETDuet (~40)	MBP-Hyp4.3; HcaF-HcaD	14+16; Fig. 4
15	pET-4.4-FD	pETDuet (~40)	MBP-Hyp4.4; HcaF-HcaD	15+16; Fig 5
16	pACYC-M	pETDuet (~40)	(empty); ProcM	See above
17	pRSF-3.1-M	pRSFDuet (>100)	MBP-Hyp3.1; ProcM	17+18; Fig. S8
18	pET-F-D	pETDuet (~40)	HcaF; HcaD	17+18; Fig. S8

Table S2. Nucleotide sequences. Restriction enzyme sites are underlined. F, forward; R, reverse. SDM, site-directed mutagenesis.

Primer Name	Primer sequence (5' to 3')	Purpose
AlbA F	<u>AAAAGATATCAATGTTTATAGAGCAGATGTTTCCATTTATTAATGAAAG</u>	RE cloning of pACYC-AlbA (EcoRV)
AlbA R	<u>AAAGACGTCCTAAATAAGCTGGACCACGCTCTTCT</u>	RE cloning of pACYC-AlbA (AatII)
HcaD F	<u>AAAAGATCTAATGACTCAAAATATATTACTTATAGGGGATGGC</u>	RE cloning of pET-F-D (BglIII)
HcaD R	<u>AAAAGGTACCCTATGGAAACGGGTGCGGATG</u>	RE cloning of pET-F-D (KpnI)
HcaF F	<u>AAAGGATCCAATGAGTAACCTTCCAGCACATGC</u>	RE cloning of pET-F-D (BamHI)
HcaF R	<u>AAAGCGGCCGCTCATAGACCGTCTCTCTTTGC</u>	RE cloning of pET-F-D (NotI)
MBP-Hyp3.1 (pRSF) F	<u>ATCACCACAGCCAGGATCCGAATTC</u> AATGAAAATCGAAGAAGGTAAACTGG	Gibson assembly of pRSF-3.1-ProcM (EcoRI)
MBP-Hyp3.1 (pRSF) R	GTTTCGACTTAAGCATTATGCGGCCGCTTAGCACTCACCCGCCAAT	Gibson assembly of pRSF-3.1-ProcM (NotI)
MBP-Hyp3.1 (pET) F	<u>CATCACCACAGCCAGGATCCG</u> AAAAATCGAAGAAGGTAAACTGGTAATC	Gibson assembly of pET-3.1-FD (BamHI)
MBP-Hyp3.1 (pET) R	<u>CGACTTAAGCATTATGCGGCCGCTTAGCACTCACCCGCCAATAG</u>	Gibson assembly of pET-3.1-FD (NotI)
HcaF-HcaD F	CATATGGCAGATCTCAATTG <u>GATATCAATGAGTAACCTTCCAGCACATG</u>	Gibson assembly of pET-Hyp-FD (EcoRV)
HcaF-HcaD R	<u>CCAGACTCGAGGGTACCGACGCTCTATG</u> AAACGGGTGCGG	Gibson assembly of pET-Hyp-FD (AatII)
MBP-Hyp4.1 F	<u>CATCACCACAGCCAGGATCCG</u> AAAAATCGAAGAAGGTAAACTGGTAATC	Gibson assembly of pET-4.1-FD (BamHI)
MBP-Hyp4.1 R	<u>TTAAGCATTATGCGGCCGCAAGCTTCTATGCGGGCACATTTTG</u>	Gibson assembly of pET-4.1-FD (HindIII)
MBP-Hyp2.1 F	<u>ACCATCATCACCACAGCCAGGATCC</u> TAAAAATCGAAGAAGGTAAACTGGTAATC	Gibson assembly of pET-2.1-FD (BamHI)
MBP-Hyp2.1 R	<u>CGACTTAAGCATTATGCGGCCGCTTAACGC</u> CATAGACCGAATAGACC	Gibson assembly of pET-2.1-FD (NotI)
HcaA leader F	<u>AAAGGATCCATGAATCAGTTTCAACA</u> AGAACTAC	RE cloning of MBP-tagged Hyp3.1 (BamHI)
HcaA leader (3.1) R	<u>GCGATGAGAGTTTAGATCCCAATACACAACATTACCAGT</u>	overlaps ProcA2.8
ProcA2.8 F	<u>GTTGTGTATTGGGATCTAAACTCTCATCGCC</u> AAAACTG	overlaps HcaA leader
ProcA2.8 R	<u>AAAAAGCTTTTAGCACTCACCCGCCAATAGG</u>	RE cloning of MBP-tagged Hyp3.1 (HindIII)
HcaA leader F	<u>AAAGGATCCATGAATCAGTTTCAACA</u> AGAACTAC	RE cloning of MBP-tagged Hyp4.1 (BamHI)
HcaA leader (4.1) R	<u>AGCGGCAGCATTAAGATCCCAATACACAACATTACCAGT</u>	overlaps ProcA3.3
ProcA3.3 F	<u>GTTGTGTATTGGGATCTTAATGCTGCCGCTTCTG</u>	overlaps HcaA leader
ProcA3.3 R	<u>AAAAAGCTTCTATGCGGGCACATTTTGG</u>	RE cloning of MBP-tagged Hyp4.1 (HindIII)
HcaA leader F	<u>AAAGGATCCATGAATCAGTTTCAACA</u> AGAACTAC	RE cloning of MBP-tagged Hyp2.1 (BamHI)
HcaA leader (2.1) R	<u>GACAGCTTTTTCATATCCCAATACACAACATTACCAG</u>	overlaps SboA
SboA F	<u>GTTGTGTATTGGGATATGAAAAAGCTGT</u> CATTGTAGAAAAC	overlaps HcaA leader
SboA R	<u>AAAGCGGCCGCTTACCCCATAGACCGAATAGACCTGTTGC</u>	RE cloning of MBP-tagged Hyp2.1 (NotI)
SboA BamHI F	<u>AAAGGATCCATGAAAAAGCTGT</u> CATTGTAGAAAACAAAGG	RE cloning
SboA NotI R	<u>AAAGCGGCCGCTTACCCCATAGACCGAATAGACCTGTTGC</u>	RE cloning
Hyp2.1 F	<u>ATTCGGTCTATGGCGTTAAGCGGCCGCACTCGAGCAC</u>	SDM
Hyp2.1 R	<u>CGGCCGCTTAACGCATAGACCGAATAGACCTGTTGC</u>	SDM
Hyp2.2 F	<u>ACATGCTCGATCGGAGCCCGTTGCGGTGGATGTGGTCTATCCCTGATTTTGA</u> AATTGC	SDM
Hyp2.2 R	<u>ATTTCAAAATCAGGGATAGGACCACATCCACCGCAACGGGCTCCGATCGAGCATGTTGC</u>	SDM
Hyp3.2 F	<u>AACCATGCTCCAGCTATGCCTCCATCTTATGGGA</u>	SDM

Hyp3.2 R	GGAGGCATAGCTGGAGCATGGTTATGACAGGCCG	SDM
Hyp 3.3 F	GCCTCCATCCTATCGTTGTGGTGAGTGCTAAGCGGCCGCATAATGC	SDM
Hyp 3.3 R	GCTTAGCACTCACCACAACGATAGGATGGAGGCATAGCTGGAGCATGG	SDM
Hyp4.2 F	ACGGCGGGGCCAAAATGTGCGCGCATAG	SDM
Hyp4.2 R	CACATTTTGGCCCCGCCGTAACATCCAGCCG	SDM
Hyp4.3 F	GCGGGGCCAAAGACTGCCGCGCATAGAAGCTTGGCGCCGCAT	SDM
Hyp4.3 R	TATGCGCGGAGTCTTTGGCCCCGCCGTAACATCCAGCCGTG	SDM
Hyp4.4 F	CGGGCGAGGCGTTTCCGGCATCCAAGCGGTGCTGCAC	SDM
Hyp4.4 R	CTTGGATGCCGGAACGCCCTCCGCCGTAGCGGCTTCC	SDM
Hyp1.1 Trunc F	GTATTTCGCTATGTACACCCGGTTGTAAAGCGTAAGGAGCTCTGTAAGGTTGTAACATGA	SDM
Hyp1.1 Trunc R	TCATGTTACAACCTTACAGAGCTCCTTACGCTTTACAACCGGTTACATAGCGAAATAC	SDM
Hyp1.1 F	GATTTGGTATCTGTTTCGAAGAAAGATTACGTTGCGGTCCACGCATTACAAGTATTTTC	SDM
Hyp1.1 R	GAAATACTTGTAAATGCGTGGACCGCAACGTGAATCTTTCGAAACAGATACCAAATC	SDM
Hyp4.5 F	AGCGCGTTTTCGCTGCTAAGCGGCCGCATAATGCTTAAGTGAACAGAAAGTAATC	SDM
Hyp4.5 R	GCCTGTCATAACCATGCTCCATCTATGCCTCCATCCTATAGCGCGTTTTCGCTGC	SDM

Gblock sequence synthesized (IDT) for Hyp1.1 (vector backbone, gray; HcaA leader peptide, blue; NisA leader peptide; mutation for HcaD/F thiazoline; NisA core peptide, black):

CACAGCCAGGATCCGAATTCGAGCTCGATGAATCAGTTCAACAAGAAGTACAATCATTAACCTTAATGATTATCAAACGGTAATGTTGTGATTTGGGATATGAGTACAAAAGATTTTAACCTTGGATTGGTATCTGTTTCGAAGAAAAGCGGCCGTTCCGGTCCACGCATTACAAGTATTTTCGCTATGTACACCCGGTTGTAAAACAGGAGCTCTGATGGGTTGTAACATGAAAACAGCAACTGTGCATTGTAGTATTCACGTAAGCAAATAAAAGCTTGCAGCGCCGATAATGCTTAAGTC

Translated peptide from Gblock sequence (coloring as above):

MNQFQQELQSLNLDYQTNVVYWDMS^TPKDFNLDLVS^VSKK^GGR^CGP^RITSISLCTPGCKTGALMGCNMKTATCHCSIHVS^K

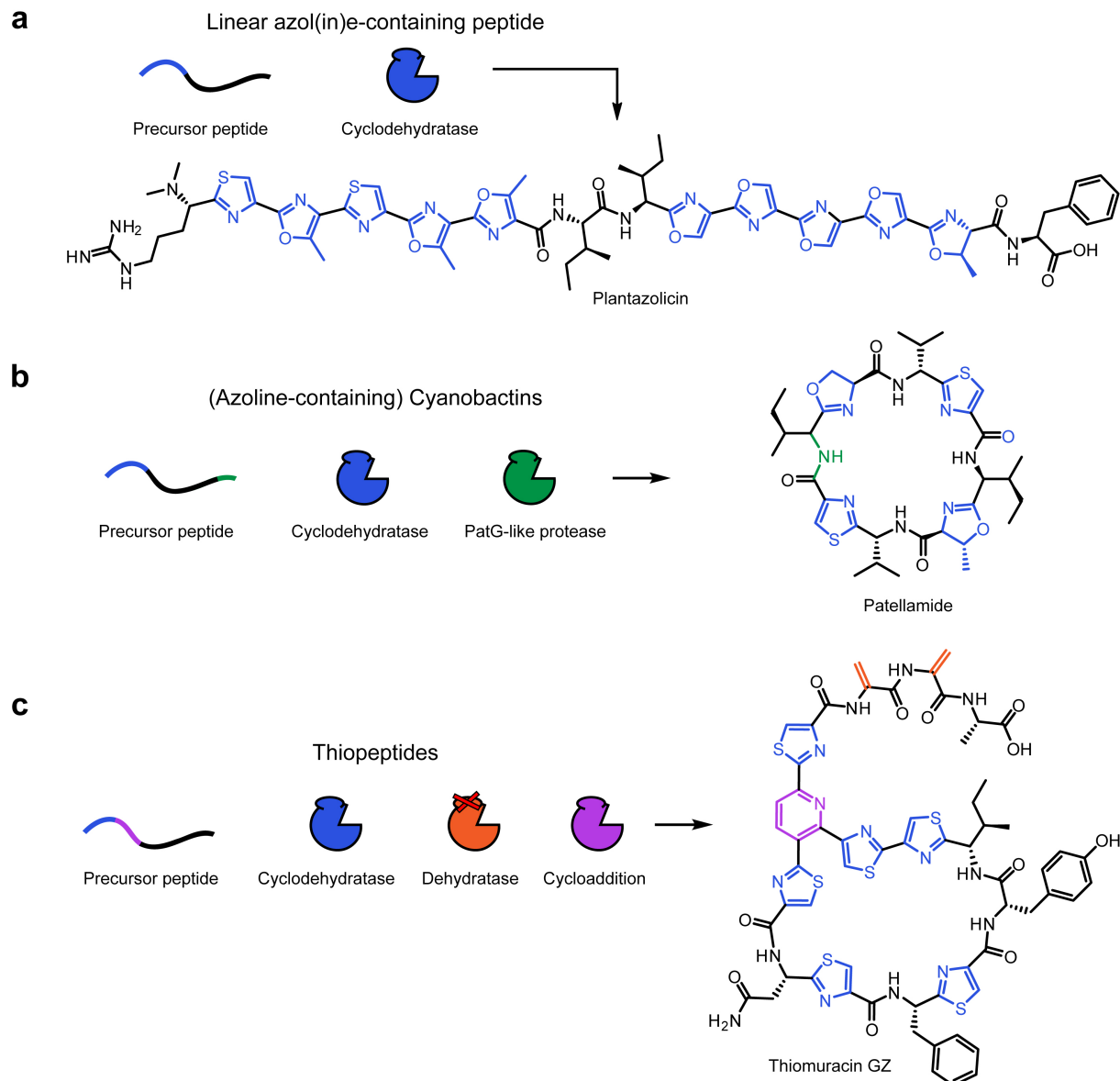


Figure S1. Natural “hybrid” RiPP biosynthetic gene clusters. (a) For linear azol(in)e-containing peptides, such as plantazolicin, the cyclodehydratase is the class-defining modifying enzyme. A tailoring enzyme also di-methylates the N-terminus upon leader peptide proteolysis. (b) Cyanobactins are defined by the presence of a PatG-like protease which recognizes a C-terminal motif to cyclize peptides after removal of the N-terminal leader region (by a PatA-like N-terminal protease). However, most cyanobactin gene clusters have acquired a cyclodehydratase and thus install two primary modifications (azolines and N-to-C macrocyclization). (c) Thiopeptides have three major modifications: azol(in)es, dehydrated amino acids, and a 6-membered nitrogen-containing heterocycle (here, pyridine). Because the cyclodehydratase and dehydratase can be found in other RiPP classes, the cycloaddition enzyme is the class-defining feature of thiopeptides. In contrast to RRE-containing and leader peptide-dependent lanthipeptide (LanB)

dehydratases,¹³ the related thiopeptide dehydratases, which also contain an RRE, are leader-independent (red “x” in figure).¹⁴

It is notable that RiPP pathways employ multiple enzymes that are dependent on certain recognition motifs and that these motifs tend to occupy distinct parts of the peptide (see panel b and c).¹⁴⁻¹⁶ Leader proteases could also be considered leader-dependent and similarly tend to bind a part of the leader not used by other enzymes.^{15,16} Nature might have evolved these physically separate binding sites to improve biosynthetic efficiency. Regardless, it appears that the recognition sequences are “plug and play” and simply need to be inserted into an existing peptide for a new enzyme to act on it.

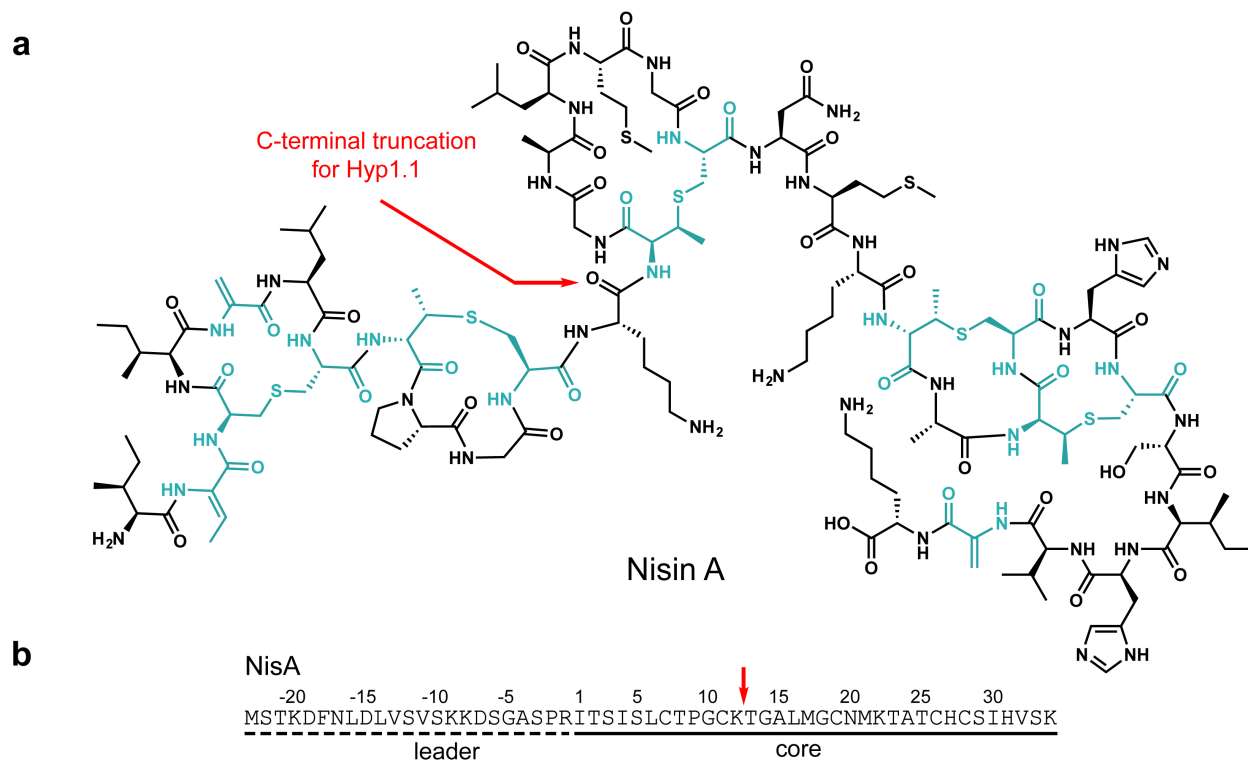


Figure S2. Structure and precursor peptide of nisin. (a) The structure of nisin A is shown with a red arrow indicating where Hyp1.1 was truncated to simplify MS/MS analysis of the modified core peptide. (b) The NisA precursor peptide sequence is shown with marked leader and core regions. The C-terminal region of the leader peptide is not required for binding or processing.^{17,18}

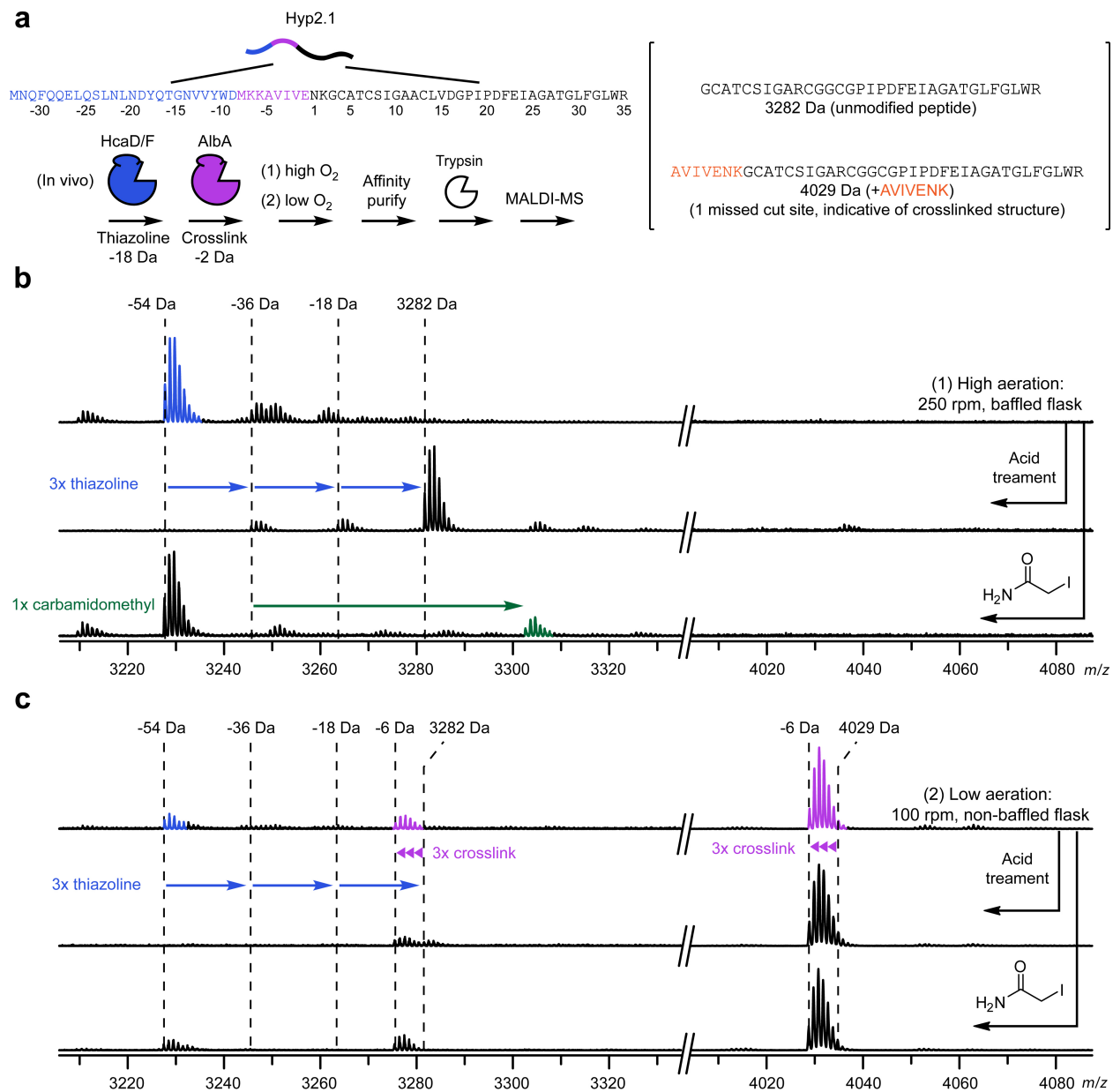
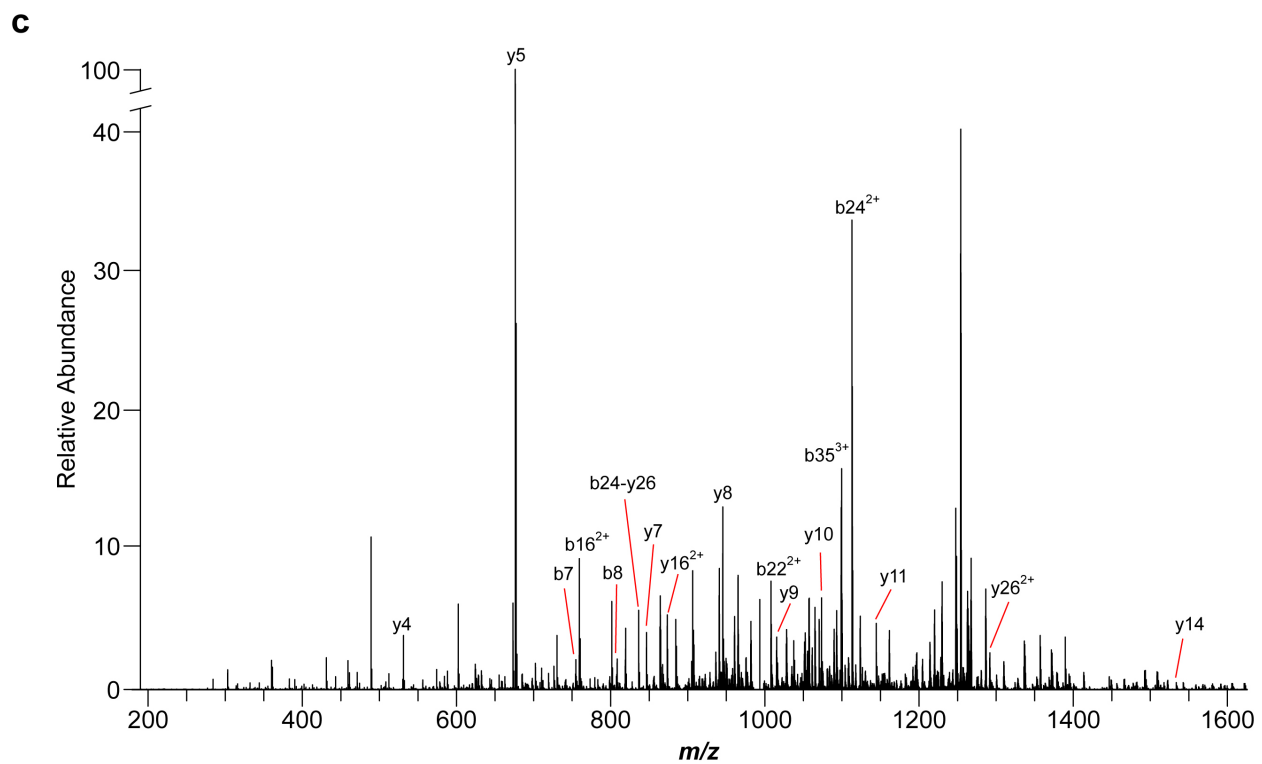
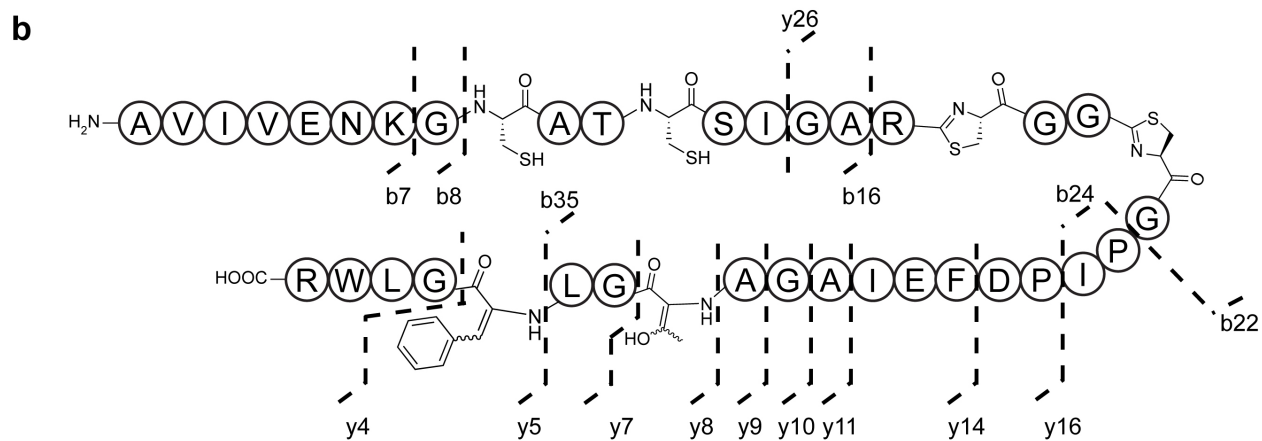
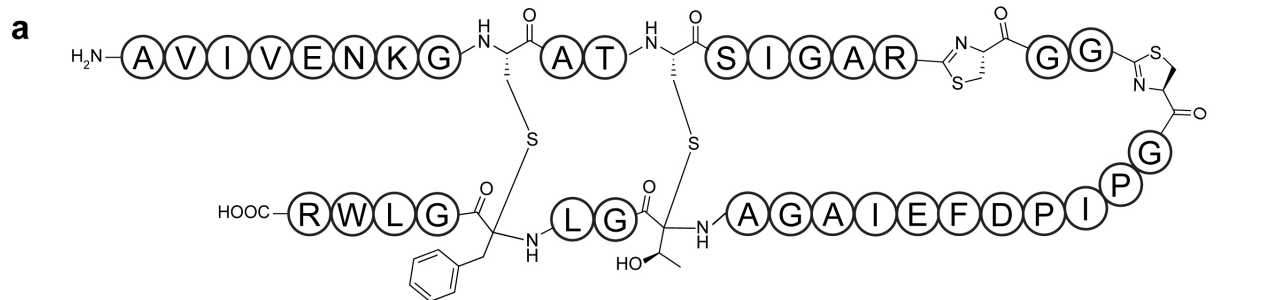


Figure S4. Hyp2.1 co-expression with HcaD/F and AlbA at high and low aeration. (a) Overview of experimental procedure. Hyp2.1 was expressed in *E. coli* with HcaD/F (pET-2.1-FD) and AlbA (pACYC-AlbA) at high or low aeration.^{6,21} (b) Under high aeration (250 rpm, baffled flasks), only thiazoline-containing products were detected. The primary product contained 3 thiazolines with a minor 2 thiazoline-containing species also detected based on acid hydrolysis and iodoacetamide labeling. (c) With low aeration (100 rpm, non-baffled flask), the predominant signal (4023 Da) corresponds to the peptide with three C α -S crosslinks based on lack of iodoacetamide labeling, but a low intensity thiazoline-containing species was observed at lower mass range because trypsin cuts more readily at Lys2 in the non-crosslinked products.



d

Ion	Theoretical mass (Da)	Observed mass (Da)	Error (ppm)
b7 ⁺	754.4458	754.4453	0.6
b16 ²⁺	759.3762	759.3739	3.1
b22 ²⁺	1007.9575	1007.9572	0.4
b24 ²⁺	1113.0262	1113.0250	1.1
b24-y26 ⁺	836.3654	836.3649	0.6
b35 ³⁺	1098.8557	1098.8551	0.5
y4 ⁺	531.3038	531.3035	0.5
y5 ⁺	676.3566	676.3562	0.6
y7 ⁺	846.4621	846.4615	0.7
y8 ⁺	945.4941	945.4935	0.7
y9 ⁺	1016.5312	1016.5304	0.8
y10 ⁺	1073.5527	1073.5522	0.5
y11 ⁺	1144.5898	1144.5888	0.9
y14 ⁺	1533.7849	1533.7836	0.8
y16 ²⁺	873.4359	873.4353	0.7
y26 ²⁺	1291.1150	1291.1135	1.1

Figure S5. MS/MS of thiazoline-modified sactipeptide Hyp2.2. (Previous page) (a) Structure of modified Hyp2.2. (b) Even at low collision energies, thioether crosslinks (thioamidals) are known to undergo elimination to form the corresponding dehydroamino acid.²¹ This enables localization of the crosslinked residues by the characteristic -2 Da at the acceptor amino acid. Fragments identified in panel are mapped onto the structure. (c) MS/MS fragmentation spectrum for Hyp2.2 annotated with identified ions. (Current page) (d) Table of predicted and observed m/z values for ions observed in panel c.

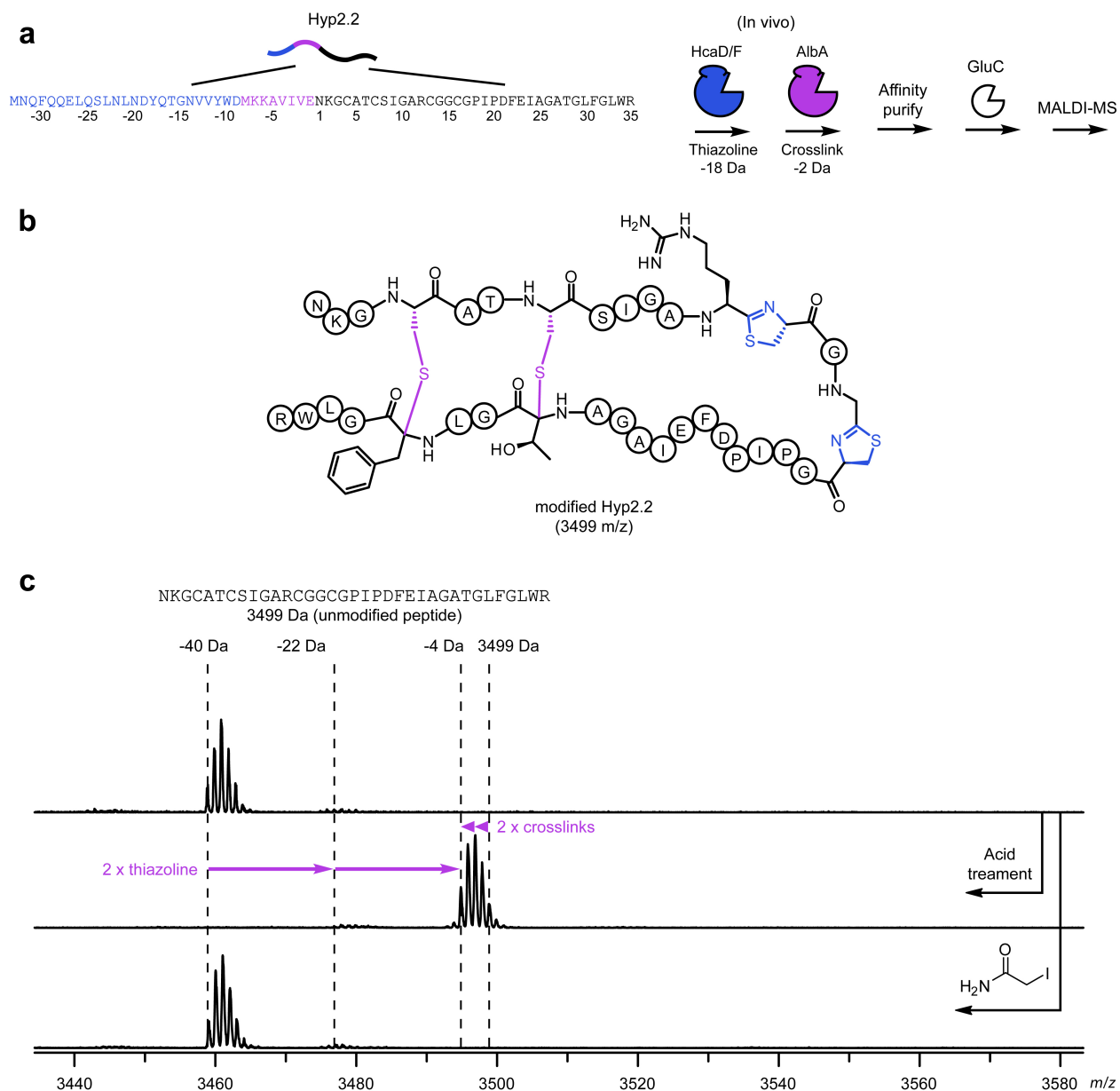


Figure S6. GluC digestion of thiazoline-modified and thioether-crosslinked Hyp 2.2. (a) Experimental overview. Hyp2.2 was expressed with HcaD/F (pET-2.2-HcaD/F) and AlbA (pACYC-AlbA) in *E. coli*. (b) Deduced structure of modified Hyp2.2 after treatment with GluC. (c) MALDI-TOF-MS analysis of modified peptide after GluC treatment and chemical derivatization. No digestion occurred at the internal Glu residue of the crosslinked peptide, supporting the proposed topology.

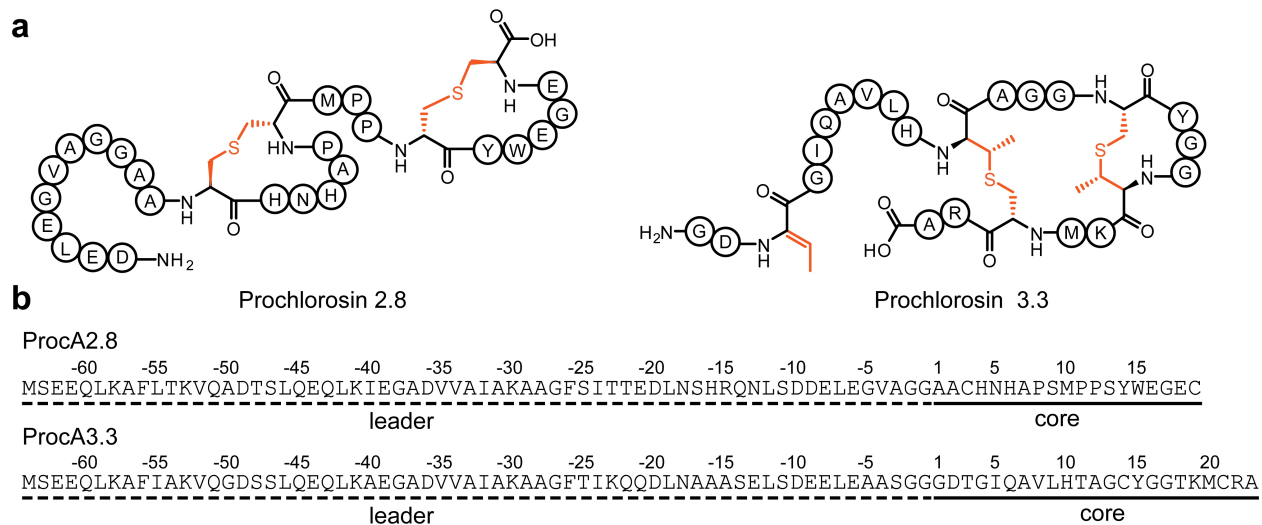


Figure S7. Structures and precursor peptides of two prochlorosins. (a) Structure of prochlorosin 2.8 and 3.3 with posttranslational modifications catalyzed by ProcM colored orange. (b) ProcM has over 30 different precursor peptides.²² The sequence of the ProcA2.8 and ProcA3.3 precursor peptides are displayed with their leader and core regions. Only the C-terminal portion of these peptides are required for processing by ProcM,²³ and in general LanM enzymes appear to bind the region of the leader peptide closest to the core peptide.²⁴

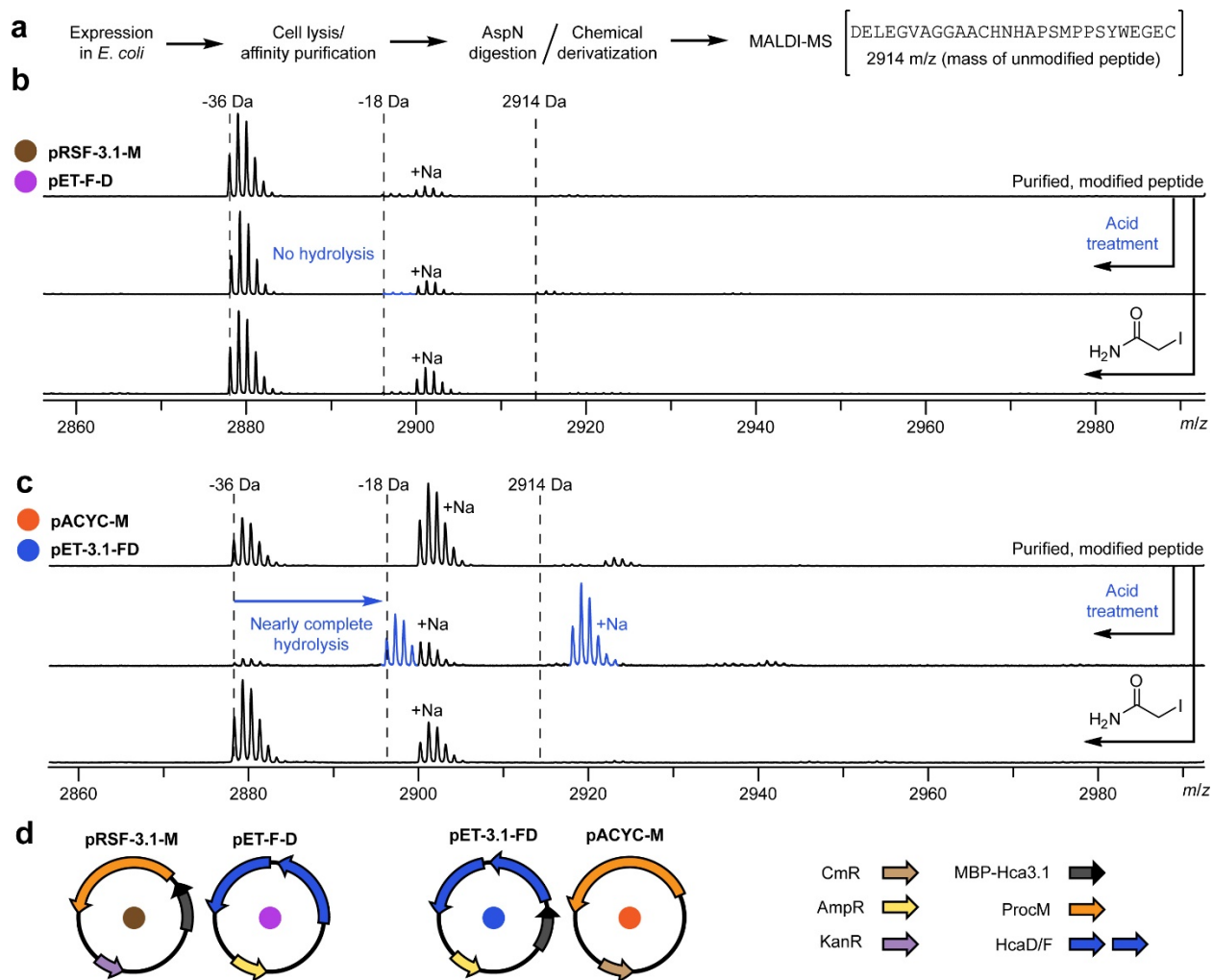


Figure S8. Optimization of HcaD/F-ProcM co-expression and plasmid design. (a) Experimental overview. (b) Expression of Hyp3.1 and ProcM on the same plasmid (pRSF-3.1-M) with HcaD/F (pET-F-D) resulted in only lanthionine formation as assessed by MALDI-TOF-MS. (c) Placing ProcM on a lower copy number plasmid (pACYC) and moving HcaD/F to the same plasmid as Hyp3.1 gave primarily a thiazoline-lanthionine product; however, a minor two lanthionine product was also detected (species at -36 Da that remains after acid treatment). (d) Legend and design of plasmids constructed for this experiment (Table S1). CmR, AmpR, and KanR are chloramphenicol, ampicillin, and kanamycin resistance markers.

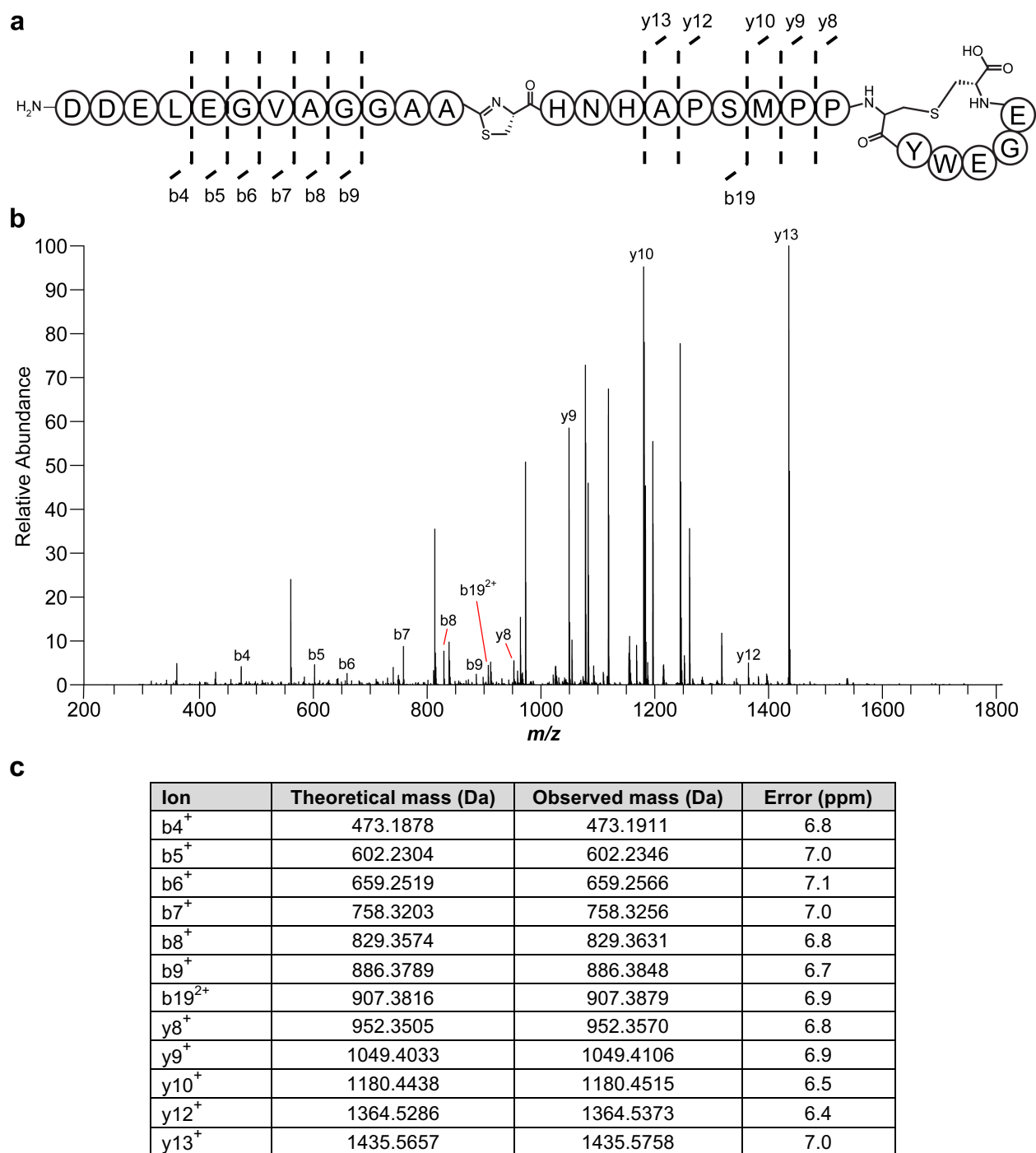


Figure S9. MS/MS fragmentation of thiazoline/lanthionine in modified Hyp3.1. (a) Structure of the thiazoline-lanthionine modified Hyp3.1 product. Although Ser9 is normally dehydrated by ProcM, thiazoline formation may inhibit dehydration at this site. Dashed lines indicate identified fragments in the mass spectrum. (b) MS/MS fragmentation spectrum for modified Hyp3.1 annotated with identified ions. (c) Table of predicted and observed m/z values for ions observed in panel b.

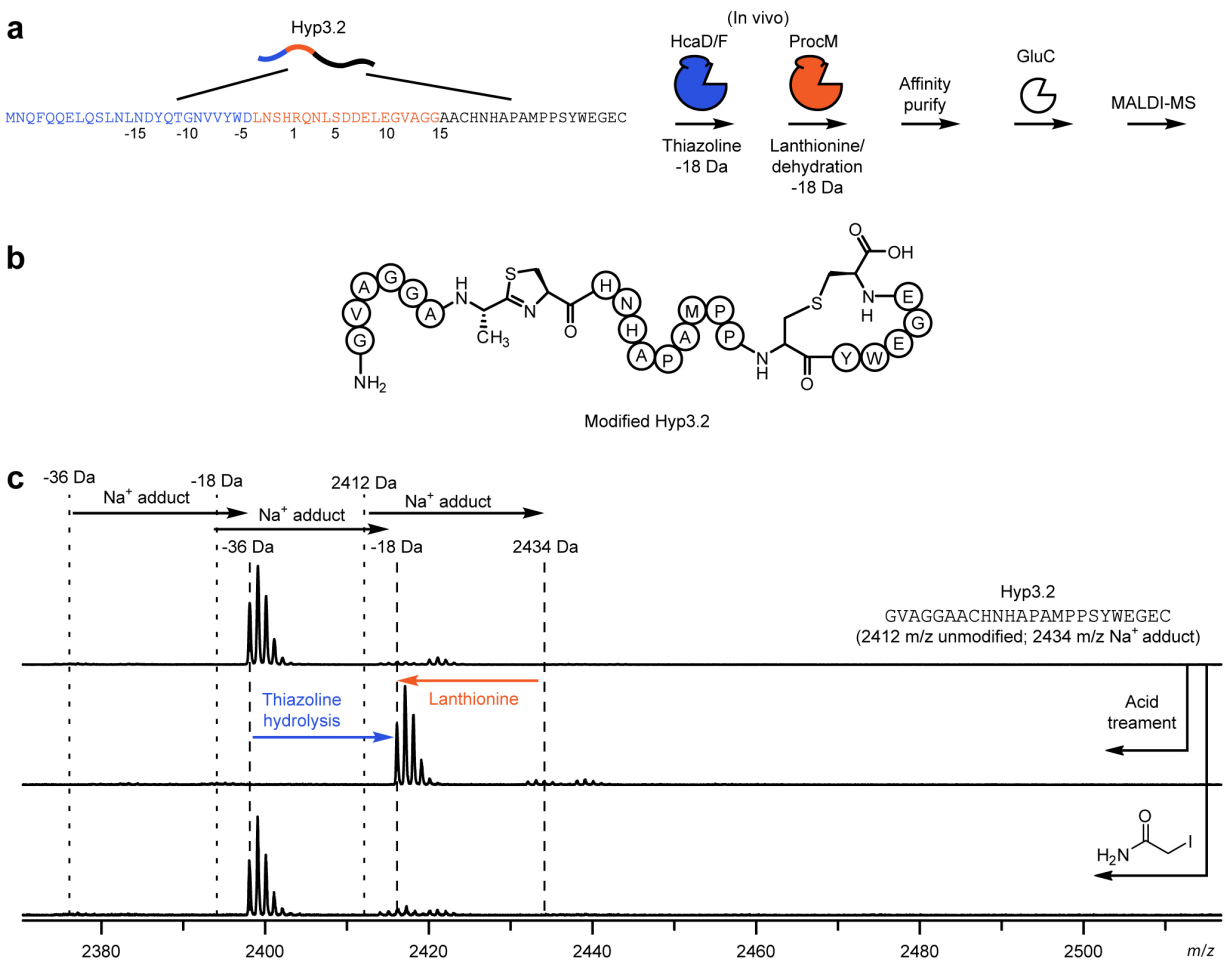
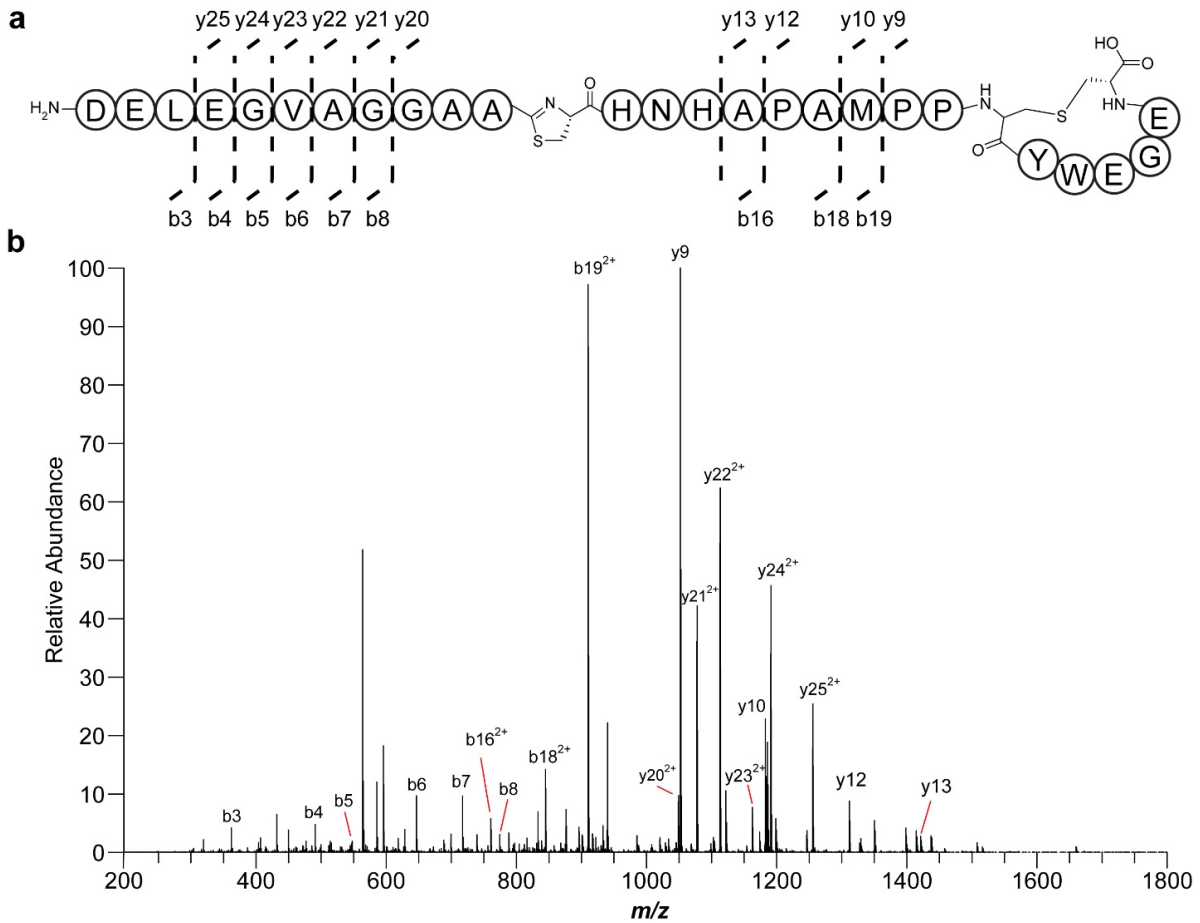


Figure S10. MALDI-TOF-MS analysis of thiazoline/lanthionine modified Hyp3.2. Compared to Hyp3.1, Hyp3.2 carries a Ser9Ala substitution. (a) Experimental overview. Hyp3.2 was co-expressed with HcaD/F (pET-3.2-FD) and ProcM (pACYC-M) in *E. coli*. (b) Deduced structure of modified Hyp3.2. (c) MALDI-TOF-MS analysis confirms the presence of a thiazoline based on the +18 Da shift upon mild acid treatment (blue arrow). The lack of iodoacetamide labeling indicates that the other Cys formed a lanthionine (orange arrow). All ions here are sodiated. The lack of GluC digestion at the two Glu near the C-terminus and the MS/MS data in Figure S11 support the proposed structure.



c

Ion	Theoretical mass (Da)	Observed mass (Da)	Error (ppm)
b3 ⁺	358.1609	358.1629	5.6
b4 ⁺	487.2035	487.2062	5.7
b5 ⁺	544.2249	544.2280	5.7
b6 ⁺	643.2934	643.2970	5.7
b7 ⁺	714.3305	714.3345	5.7
b8 ⁺	771.3519	771.3563	5.7
b16 ²⁺	757.8257	757.8298	5.4
b18 ²⁺	841.8706	841.8752	5.5
b19 ²⁺	907.3909	907.3961	5.7
y9 ⁺	1049.4033	1049.4089	5.3
y10 ⁺	1180.4438	1180.4502	5.4
y12 ⁺	1348.5337	1348.5415	5.8
y13 ⁺	1419.5708	1419.5781	5.2
y20 ²⁺	1046.4166	1046.4223	5.5
y21 ²⁺	1074.9273	1074.9330	5.3
y22 ²⁺	1110.4459	1110.4517	5.3
y23 ²⁺	1159.9800	1159.9862	5.3
y24 ²⁺	1188.4908	1188.4972	5.4
y25 ²⁺	1253.0121	1253.0194	5.8

Figure S11. MS/MS fragmentation of thiazoline/lanthionine in modified Hyp3.2 digested with AspN. (Previous page) (a) Structure of the thiazoline-lanthionine modified Hyp3.2 product. Dashed lines indicate identified fragments in the mass spectrum. (b) MS/MS fragmentation spectrum for modified Hyp3.2 annotated with identified ions. (c) Table of predicted and observed m/z values found for ions observed in panel b.

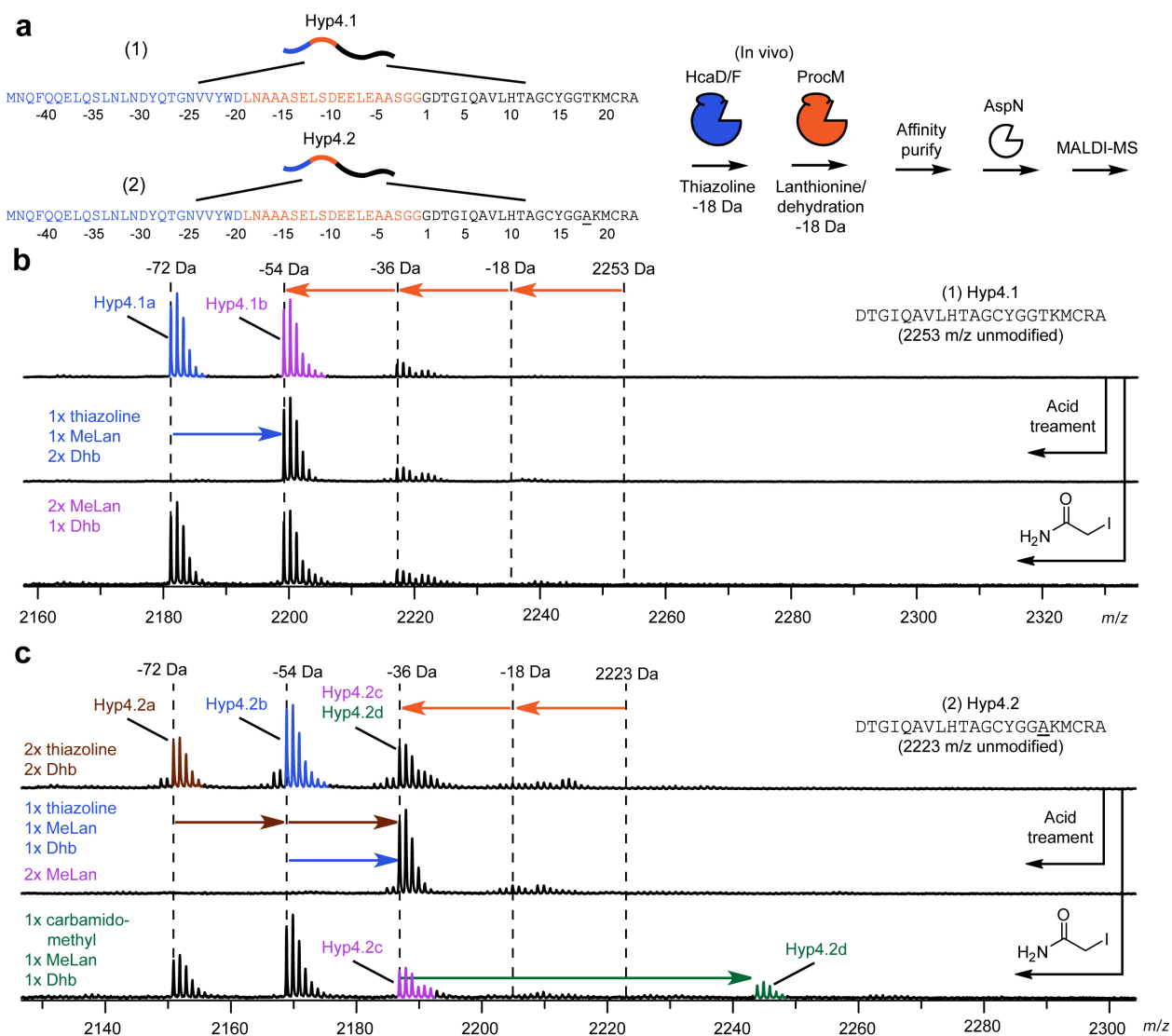
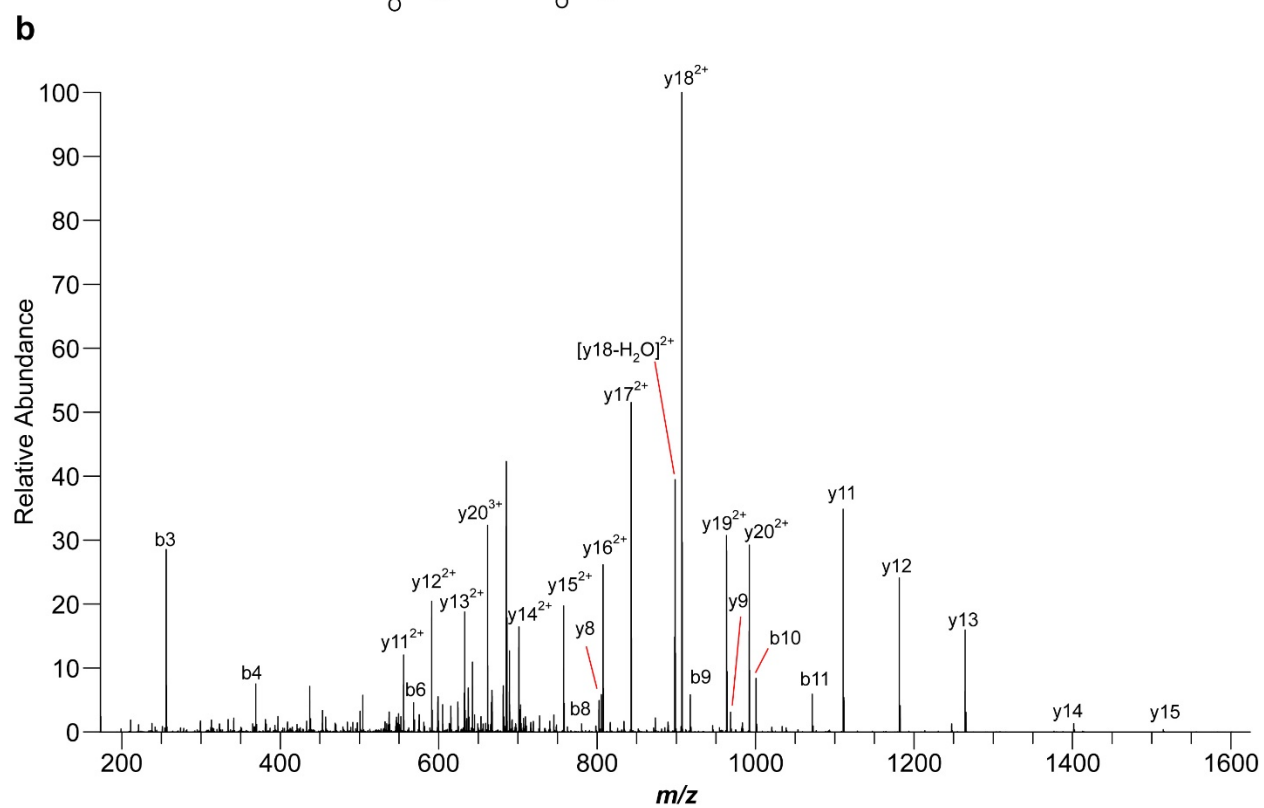
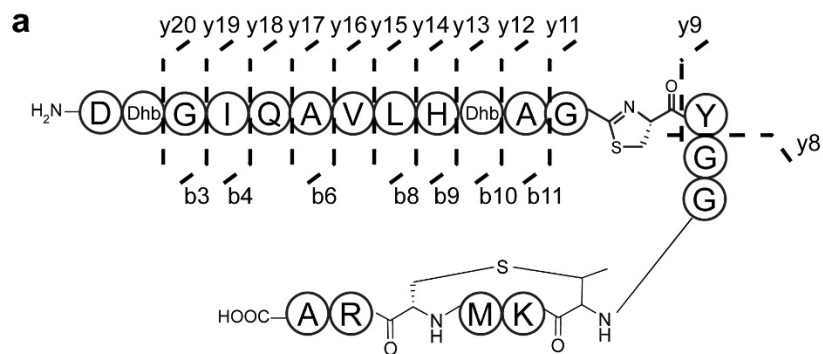


Figure S12. Thiiazoline and lanthionine product mixtures produced with Hyp4.1 and Hyp4.2. (a) Experimental overview. (b) When Hyp4.1 was co-expressed with HcaD/F (pET-4.1-FD) and ProcM (pACYC-M), two main products were detected. Hyp4.1a has one thiiazoline and lanthionine (see Figure S15 for MS/MS), but the lack of mild acid hydrolysis and lack of iodoacetamide labeling suggested that Hyp4.1b displayed modifications akin to native prochlorosin 3.3. (c) With the Thr18Ala substitution in Hyp4.2 (underlined, panel a), co-expression of Hyp4.2 with HcaD/F (pET-4.2-FD) and ProcM (pACYC-M) produced multiple products indicating there was little preference for the modification order. Hyp4.2a contained two thiazolines, Hyp4.2b contained one thiiazoline, while the other products were not susceptible to mild acid hydrolysis. Hyp4.2c likely contains two lanthionines while Hyp4.2d displayed a free Cys based on iodoacetamide labeling. Blue/brown arrows indicate acid hydrolysis (+18 Da). Orange arrows indicate Dhb/MeLan formation (-18 Da). Green arrow indicates carbamidomethylation upon reaction with iodoacetamide (+57 Da).

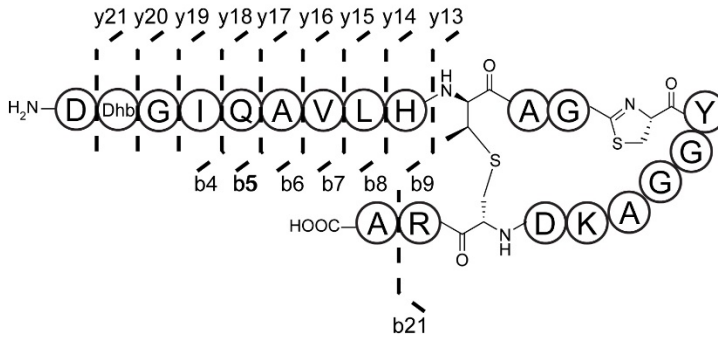


C

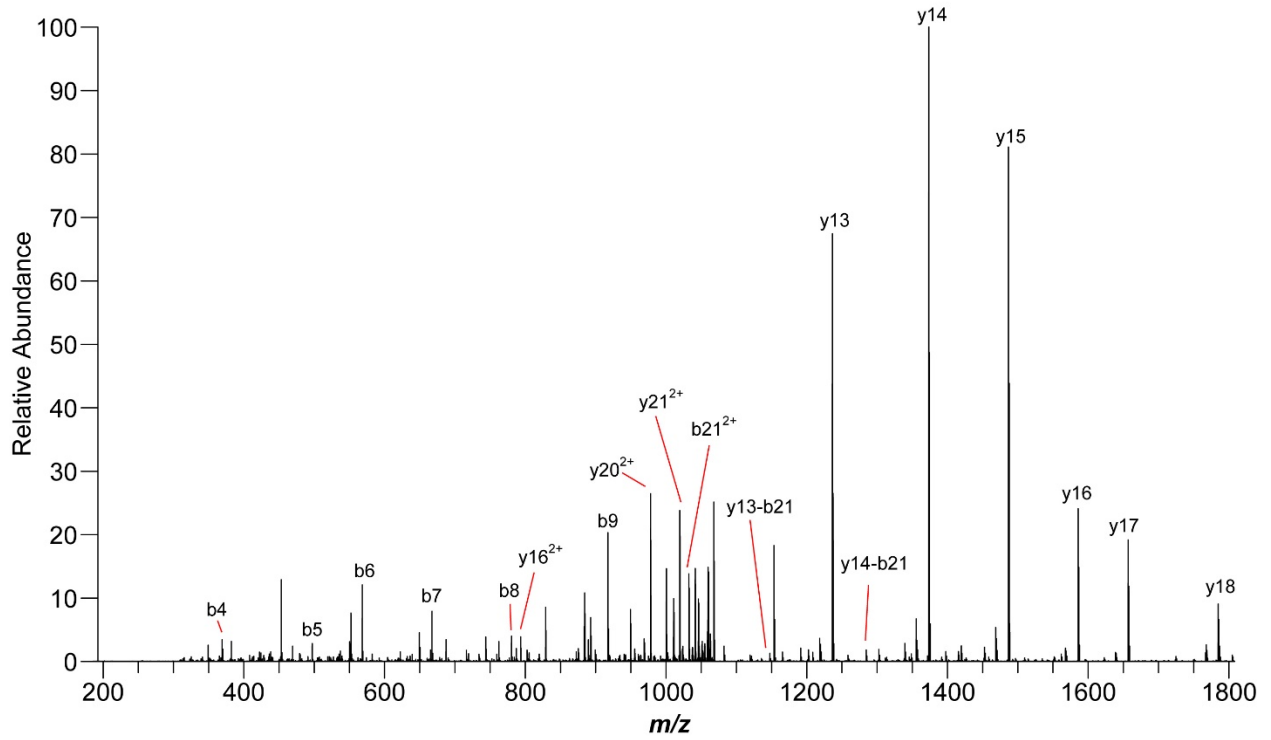
Ion	Theoretical mass (Da)	Observed mass (Da)	Error (ppm)
b3 ⁺	256.0928	256.0940	4.6
b4 ⁺	369.1769	369.1785	4.4
b6 ⁺	568.2726	568.2741	4.3
b8 ⁺	780.4250	780.4285	4.4
b9 ⁺	917.4839	917.4879	4.4
b10 ⁺	1000.5255	1000.5211	4.4
b11 ⁺	1071.5582	1071.5628	4.3
y11 ⁺	1110.4642	1110.4692	4.5
y11 ²⁺	555.7357	555.7383	4.6
y12 ⁺	1181.5013	1181.5063	4.3
y12 ²⁺	591.2543	591.2570	4.7
y13 ⁺	1264.5384	1264.5439	4.3
y13 ²⁺	632.7728	632.7758	4.7
y14 ⁺	1401.5973	1401.6038	4.6
y14 ²⁺	701.3023	701.3056	4.7
y15 ⁺	1514.6814	1514.6889	5.0
y15 ²⁺	757.8443	757.8479	4.7
y16 ²⁺	807.3785	807.3821	4.5
y17 ²⁺	842.8971	842.9009	4.5
y18 ²⁺	906.9264	906.9303	4.4
[y18-H ₂ O] ²⁺	897.9211	897.9251	4.5
y19 ²⁺	963.4684	963.4727	4.5
y20 ²⁺	991.9791	991.9836	4.5
y20 ³⁺	661.6552	661.6584	4.8

Figure S13. MS/MS fragmentation of modified Hyp4.1a. (Previous Page) (a) Modified structure of the Dhb, thiazoline, and lanthionine modified Hyp4.1a. Dashed lines indicate identified fragments in the mass spectrum. (b) MS/MS fragmentation spectrum for modified Hyp4.1a annotated with identified ions. (Current page) (c) Table of predicted and observed m/z values for ions in panel b.

a



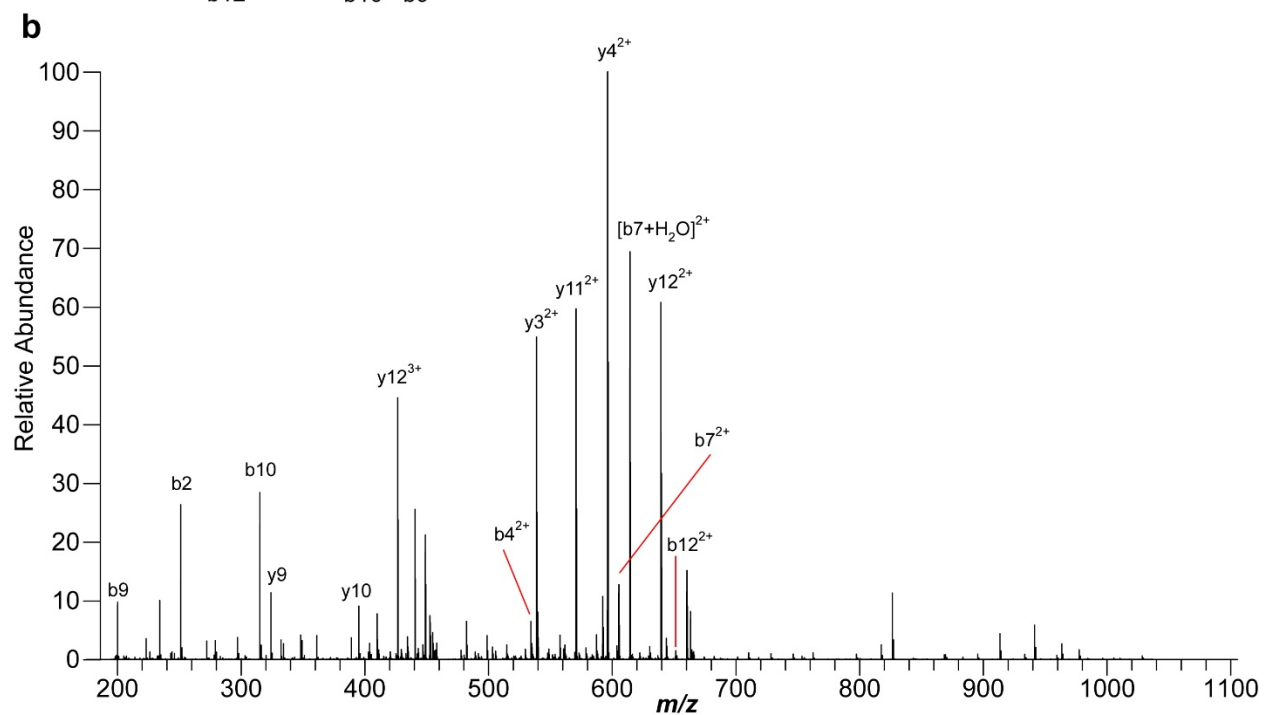
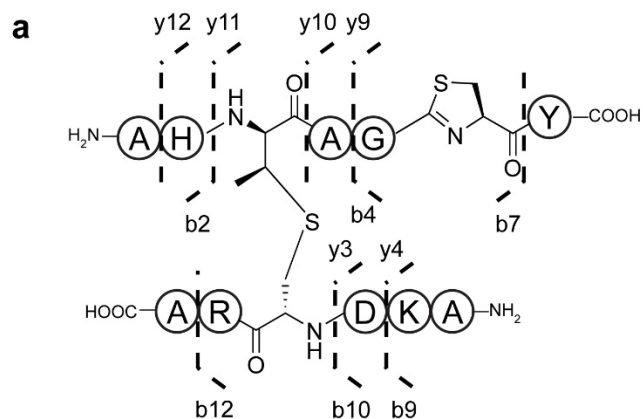
b



c

Ion	Theoretical mass (Da)	Observed mass (Da)	Error (ppb)
b3 ⁺	256.0928	256.0927	312.4
b4 ⁺	369.1769	369.1767	541.7
b5 ⁺	497.2354	497.2353	281.6
b6 ⁺	568.2726	568.2725	176.0
b7 ⁺	667.3410	667.3408	269.7
b9 ⁺	917.4839	917.4834	566.8
b10 ⁺	1000.5211	1000.5206	479.8
b11 ⁺	1071.5582	1071.5576	559.9
y4 ⁺	462.1952	462.1950	454.4
y5 ⁺	590.2901	590.2900	288.0
y8 ⁺	775.3702	775.3698	451.4
y11 ⁺	1080.4536	1080.4530	536.8
y11 ²⁺	540.7304	540.7304	147.9
y12 ⁺	1151.4907	1151.4899	677.4
y12 ²⁺	576.2490	576.2488	329.7
y13 ⁺	1234.5278	1234.5279	48.6
y13 ²⁺	617.7676	617.7675	161.9
y14 ⁺	1371.5867	1371.5861	444.7
y14 ²⁺	686.2970	686.2968	320.6
y15 ⁺	1484.6708	1484.6703	107.8
y15 ²⁺	742.8390	742.8389	175.0
y16 ²⁺	792.3732	792.3730	290.3
y17 ²⁺	827.8918	827.8915	374.4
y18 ²⁺	891.9211	891.9206	583.0
y19 ²⁺	948.4631	948.4626	601.0
y20 ²⁺	976.9739	976.9736	245.7
y20 ³⁺	651.6517	651.6516	168.8

Figure S14. MS/MS fragmentation of modified Hyp4.3a. (Previous page) (a) Structure of the Dhb, thiazoline, and lanthionine modified Hyp4.3. Dashed lines indicate identified fragments in the mass spectrum. (b) MS/MS fragmentation spectrum for modified Hyp4.3 annotated with identified ions. (c) Table of predicted and observed m/z values for ions in panel b.



c

Ion	Theoretical mass (Da)	Observed mass (Da)	Error (ppm)
$b2^+$	251.1503	251.1516	5.4
$b4^{2+}$	534.2744	534.2773	5.4
$b7^{2+}$	605.2844	605.2876	5.2
$[b7+H_2O]^{2+}$	614.2897	614.2929	5.2
$b9^+$	200.1394	200.1405	5.7
$b10^+$	315.1663	315.1679	5.1
$b12^{2+}$	651.2975	651.3010	5.3
$y3^{2+}$	538.7419	538.7448	5.4
$y4^{2+}$	596.2553	596.2586	5.4
$y9^+$	324.1013	324.1028	4.9
$y10^+$	395.1384	395.1403	5.0
$y11^{2+}$	570.7499	570.7528	5.1
$y12^{2+}$	639.2793	639.2827	5.3
$y12^{3+}$	426.5220	426.5242	5.1

Figure S15 MS/MS fragmentation of modified Hyp4.3a after thermolysin digestion. (Previous page)
(a) Structure of the lanthionine ring fragment of Hyp4.3 after digestion by thermolysin. Dashed lines indicate identified fragments in the mass spectrum. (b) MS/MS fragmentation spectrum for lanthionine ring of Hyp4.3 after digestion and HPLC-purification annotated with identified ions. (c) Table of predicted and observed m/z values of ions seen in panel b.

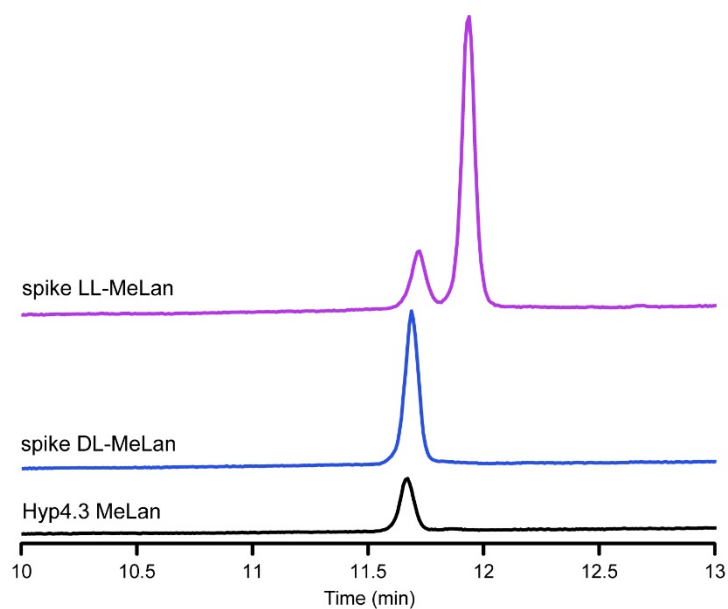
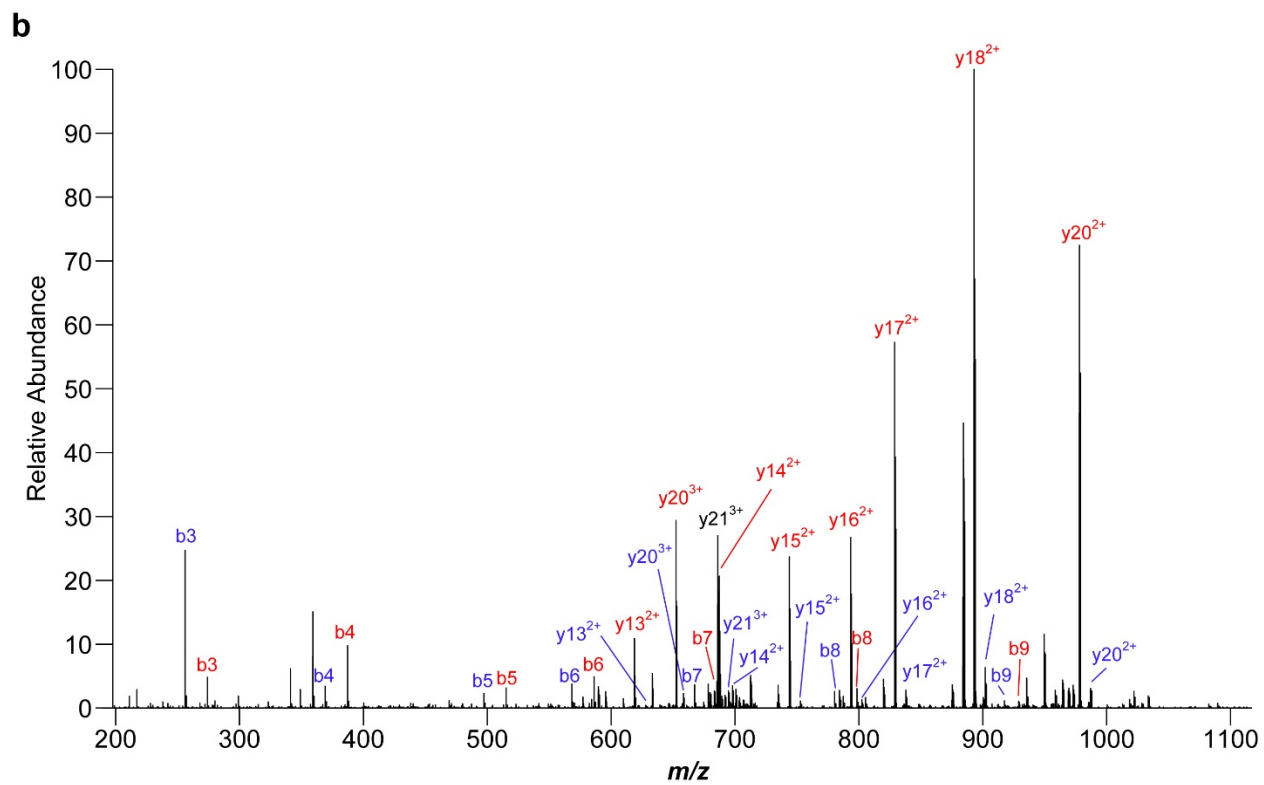
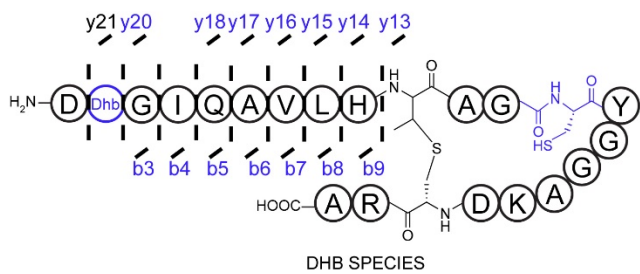
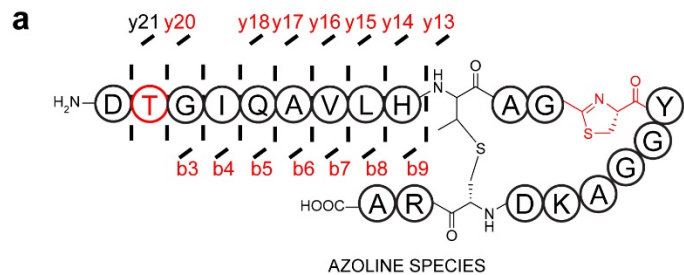


Figure S16. GC-MS analysis of Hyp3.3 MeLan. After hydrolysis and derivatization, the MeLan of Hyp3.3 co-eluted when spiked with authentic DL-MeLan but not with LL-MeLan, indicating that the stereochemistry of the lanthionine in Hyp3.3 is DL as in the native prochlorosins.¹⁰



c

Azoline species			
Ion	Theoretical mass (Da)	Observed mass (Da)	Error (ppm)
b3 ⁺	274.1034	274.1045	4.3
b4 ⁺	387.1874	387.1890	4.0
b5 ⁺	515.2460	515.2483	4.4
b6 ⁺	586.2831	586.2856	4.2
b7 ⁺	685.3515	685.3543	4.0
b8 ⁺	798.4356	798.4389	4.1
b9 ⁺	935.4945	935.4983	4.1
y13 ²⁺	618.7661	618.7687	4.3
y14 ²⁺	687.2955	687.2984	4.1
y15 ²⁺	743.8376	743.8407	4.2
y16 ²⁺	793.3718	793.3749	4.0
y17 ²⁺	828.8903	828.8936	4.0
y18 ²⁺	892.9196	892.9230	3.8
y20 ²⁺	977.9724	977.9762	3.9
y21 ³⁺	685.9999	686.0027	4.1

Dhb species			
Ion	Theoretical mass (Da)	Observed mass (Da)	Error (ppm)
b3 ⁺	256.0928	256.0939	4.1
b4 ⁺	369.1769	369.1784	4.2
b5 ⁺	497.2354	497.2374	3.9
b6 ⁺	568.2726	568.2748	4.0
b7 ⁺	667.3410	667.3437	4.1
b8 ⁺	780.4250	780.4283	4.2
b9 ⁺	917.4839	917.4877	4.1
y13 ²⁺	627.7713	627.7740	4.2
y14 ²⁺	696.3008	696.3041	4.7
y15 ²⁺	752.8428	752.8457	3.8
y16 ²⁺	802.3770	802.3799	3.6
y17 ²⁺	837.8956	837.8989	4.0
y18 ²⁺	901.9249	901.9284	3.9
y20 ²⁺	986.9776	986.9814	3.8
y21 ³⁺	685.9999	686.0027	4.1

Figure S17. MS/MS fragmentation of Hyp4.3 minor products. (Previous page) (a) Structure of two minor products (azoline or Dhb) after expression of Hyp4.3 with HcaD/F (pET-4.3-FD) and ProcM (pACYC-M). A third product, a species containing two lanthionines, also formed (from a Michael-like addition within in the Dhb product) based on MALDI-TOF-MS analysis (Figure 3c), but did not undergo fragmentation, likely owing to the lanthionines. Dashed lines indicate identified fragments. (b) Annotated MS/MS spectrum for minor products. (c) Table of predicted and observed m/z values for ions from panel b. Red (azoline) and blue (Dhb) colors indicate the two species.

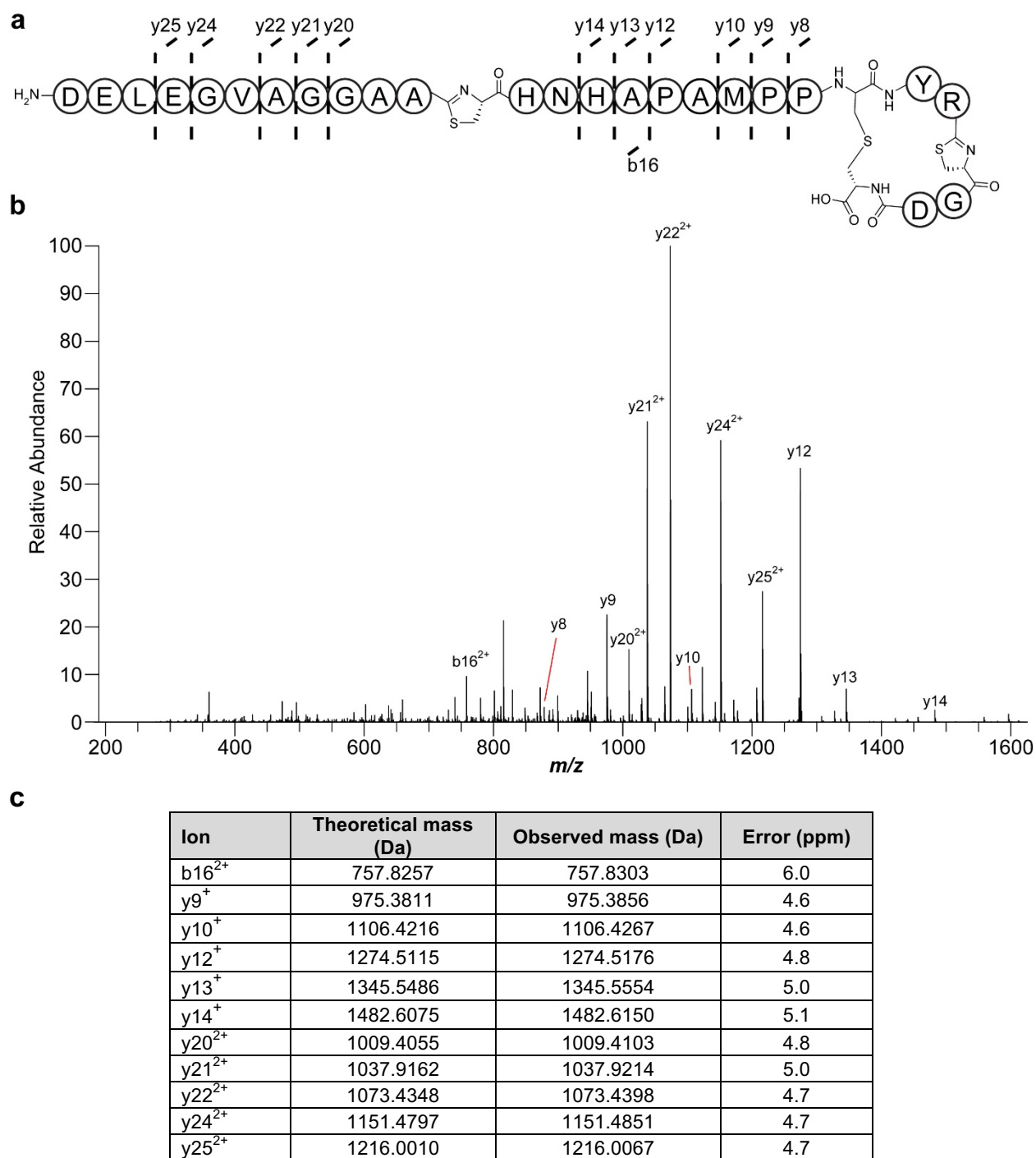


Figure S18. MS/MS fragmentation of thiazoline/lanthionine modified Hyp3.3. (a) Structure of the modified Hyp3.3 product containing two thiazolines and one lanthionine. Dashed lines indicate identified fragments in the mass spectrum. (b) MS/MS fragmentation spectrum for modified Hyp3.3 annotated with identified ions. (c) Table of predicted and observed m/z values for ions observed in panel b.

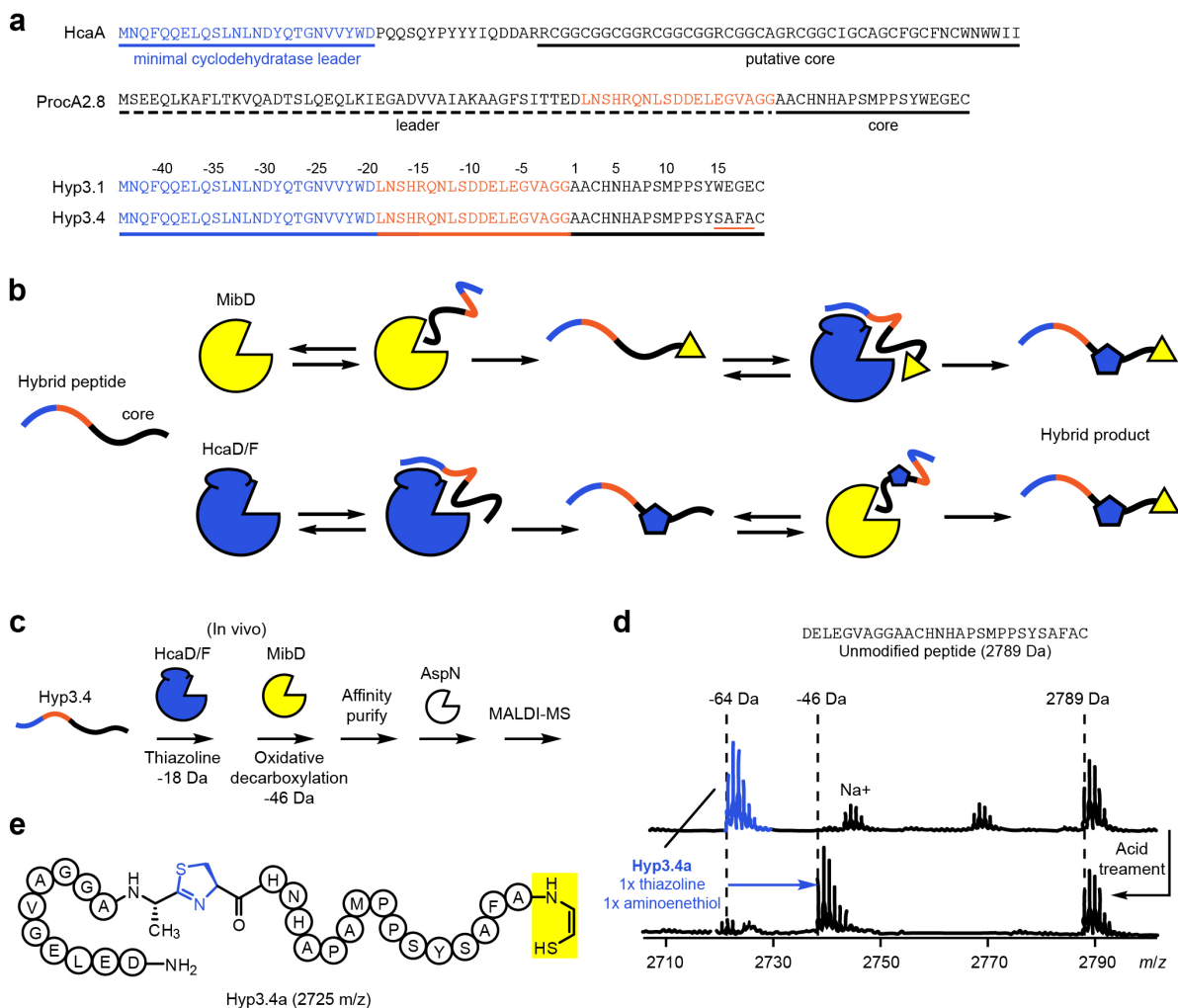


Figure S19. Design and production of decarboxylated linear azol(in)e-containing peptide. (a) A hybrid peptide was designed that would enable modification by HcaD/F and the leader-independent tailoring enzyme MibD from *Microbispora* sp. 107891. MibD is a LanD enzyme and carries out oxidative decarboxylation of C-terminal Cys to the corresponding aminoenethiolate, and its preferred core sequence is S-(F/W/N)-(N/C)-S-(F/Y/W/N)-C-C.⁸ This motif was mimicked by changing the C-terminus of the peptide to SAFAC to create Hyp3.4. Although the ProcM leader region was present, ProcM was not used in this experiment. (b) Anticipated hybrid biosynthesis. As both thiazoline and decarboxylation are smaller modifications occurring on different ends of the core peptide, the enzymes can presumably act in any order. (c) Overview of experiment. Hyp3.4 was co-expressed with HcaD/F (pET-3.4-FD) and MibD in pCDFDuet (see plasmid list in Table S1). The peptide was purified, digested with AspN, and analyzed by MALDI-TOF-MS. (d) The mass spectrum shows a several ions, but the most intense peak (labeled Hyp3.4a) corresponded to the desired hybrid product. (e) Deduced structure of the hybrid Hyp3.4a product after AspN digestion.

References

- (1) Dunbar, K. L.; Tietz, J. I.; Cox, C. L.; Burkhart, B. J.; Mitchell, D. A. Identification of an Auxiliary Leader Peptide-Binding Protein Required for Azoline Formation in Ribosomal Natural Products. *J. Am. Chem. Soc.* **2015**, *137* (24), 7672-7677.
- (2) Shi, Y.; Yang, X.; Garg, N.; van der Donk, W. A. Production of Lantipeptides in *Escherichia coli*. *J. Am. Chem. Soc.* **2011**, *133* (8), 2338-2341.
- (3) Yang, X.; van der Donk, W. A. Post-translational introduction of D-alanine into ribosomally synthesized peptides by the dehydroalanine reductase NpnJ. *J. Am. Chem. Soc.* **2015**, *137* (39), 12426-12429.
- (4) Ortega, M. A.; Cogan, D. P.; Mukherjee, S.; Garg, N.; Li, B.; Thibodeaux, G. N.; Maffioli, S. I.; Donadio, S.; Sosio, M.; Escano, J. et al. Two Flavoenzymes Catalyze the Post-Translational Generation of 5-Chlorotryptophan and 2-Aminovinyl-Cysteine during NAI-107 Biosynthesis. *ACS Chem Biol* **2017**, *12* (2), 548-557.
- (5) Tolia, N. H.; Joshua-Tor, L. Strategies for protein coexpression in *Escherichia coli*. *Nat. Methods* **2006**, *3* (1), 55-64.
- (6) McDaniel, L. E.; Bailey, E. G. Effect of Shaking Speed and Type of Closure on Shake Flask Cultures. *Appl. Microbiol.* **1969**, *17* (2), 286-290.
- (7) Mukherjee, S.; van der Donk, W. A. Mechanistic studies on the substrate-tolerant lanthipeptide synthetase ProcM. *J. Am. Chem. Soc.* **2014**, *136* (29), 10450-10459.
- (8) Ortega, M. A.; Cogan, D. P.; Mukherjee, S.; Garg, N.; Li, B.; Thibodeaux, G. N.; Maffioli, S. I.; Donadio, S.; Sosio, M.; Escano, J. et al. Two flavoenzymes catalyze the post-translational generation of 5-chlorotryptophan and 2-aminovinyl-cysteine during NAI-107 biosynthesis. *ACS Chem. Biol.* **2017**, DOI:10.1021/acscchembio.6b01031 10.1021/acscchembio.6b01031.
- (9) Dunbar, K. L.; Mitchell, D. A. Insights into the mechanism of peptide cyclodehydrations achieved through the chemoenzymatic generation of amide derivatives. *J. Am. Chem. Soc.* **2013**, *135* (23), 8692-8701.
- (10) Tang, W.; van der Donk, W. A. Structural Characterization of Four Prochlorosins: A Novel Class of Lantipeptides Produced by Planktonic Marine Cyanobacteria. *Biochemistry* **2012**, *51* (21), 4271-4279.
- (11) Liu, W.; Chan, A. S.; Liu, H.; Cochrane, S. A.; Vederas, J. C. Solid supported chemical syntheses of both components of the lantibiotic lactacin 3147. *J. Am. Chem. Soc.* **2011**, *133* (36), 14216-14219.
- (12) Held, D.; Yaeger, K.; Novy, R. New coexpression vectors for expanded compatibilities in *E. coli*. *InNovations* **2003**, *18*, 4-6.
- (13) Repka, L. M.; Chekan, J. R.; Nair, S. K.; van der Donk, W. A. Mechanistic Understanding of Lanthipeptide Biosynthetic Enzymes. *Chem. Rev.* **2017**, *117* (8), 5457-5520.
- (14) Zhang, Z.; Hudson, G. A.; Mahanta, N.; Tietz, J. I.; van der Donk, W. A.; Mitchell, D. A. Biosynthetic timing and substrate specificity for the thiopeptide thiomuracin. *J. Am. Chem. Soc.* **2016**, *138* (48), 15511-15514.
- (15) Sardar, D.; Pierce, E.; McIntosh, J. A.; Schmidt, E. W. Recognition sequences and substrate evolution in cyanobactin biosynthesis. *ACS Synth. Biol.* **2015**, *4* (2), 167-176.
- (16) Yang, X.; van der Donk, W. A. Ribosomally synthesized and post-translationally modified peptide natural products: new insights into the role of leader and core peptides during biosynthesis. *Chem. Eur. J.* **2013**, *19* (24), 7662-7677.

- (17) Khusainov, R.; Moll, G. N.; Kuipers, O. P. Identification of distinct nisin leader peptide regions that determine interactions with the modification enzymes NisB and NisC. *FEBS Open Bio* **2013**, *3*, 237-242.
- (18) Plat, A.; Kluskens, L. D.; Kuipers, A.; Rink, R.; Moll, G. N. Requirements of the engineered leader peptide of nisin for inducing modification, export, and cleavage. *Appl. Environ. Microbiol.* **2011**, *77* (2), 604-611.
- (19) Wieckowski, B. M.; Hegemann, J. D.; Mielcarek, A.; Boss, L.; Burghaus, O.; Marahiel, M. A. The PqqD homologous domain of the radical SAM enzyme ThnB is required for thioether bond formation during thurincin H maturation. *FEBS Lett.* **2015**, *589* (15), 1802-1806.
- (20) Burkhardt, B. J.; Hudson, G. A.; Dunbar, K. L.; Mitchell, D. A. A prevalent peptide-binding domain guides ribosomal natural product biosynthesis. *Nat. Chem. Biol.* **2015**, *11* (8), 564-570.
- (21) Himes, P. M.; Allen, S. E.; Hwang, S.; Bowers, A. A. Production of sactipeptides in *Escherichia coli*: Probing the substrate promiscuity of subtilisin A biosynthesis. *ACS Chem. Biol.* **2016**, *11* (6), 1737-1744.
- (22) Li, B.; Sher, D.; Kelly, L.; Shi, Y.; Huang, K.; Knerr, P. J.; Joewono, I.; Rusch, D.; Chisholm, S. W.; van der Donk, W. A. Catalytic promiscuity in the biosynthesis of cyclic peptide secondary metabolites in planktonic marine cyanobacteria. *Proc. Natl. Acad. Sci. USA* **2010**, *107* (23), 10430-10435.
- (23) Zhang, Q.; Yang, X.; Wang, H.; van der Donk, W. A. High divergence of the precursor peptides in combinatorial lanthipeptide biosynthesis. *ACS Chem. Biol.* **2014**, *9* (11), 2686-2694.
- (24) Xie, L.; Miller, L. M.; Chatterjee, C.; Averin, O.; Kelleher, N. L.; van der Donk, W. A. Lacticin 481: in vitro reconstitution of lantibiotic synthetase activity. *Science* **2004**, *303* (5658), 679-681.